

The University of Southern Mississippi  
**The Aquila Digital Community**

---

Honors Theses

Honors College

---

Spring 5-2016

**Functionalizing  $\beta$ -Cyano Oligo(p-phenylene vinylene)  
Chromophores for Use in Mechanochromic Materials**

Alexander J. Wink  
*University of Southern Mississippi*

Follow this and additional works at: [https://aquila.usm.edu/honors\\_theses](https://aquila.usm.edu/honors_theses)

 Part of the [Polymer Chemistry Commons](#)

---

**Recommended Citation**

Wink, Alexander J., "Functionalizing  $\beta$ -Cyano Oligo(p-phenylene vinylene) Chromophores for Use in Mechanochromic Materials" (2016). *Honors Theses*. 357.  
[https://aquila.usm.edu/honors\\_theses/357](https://aquila.usm.edu/honors_theses/357)

This Honors College Thesis is brought to you for free and open access by the Honors College at The Aquila Digital Community. It has been accepted for inclusion in Honors Theses by an authorized administrator of The Aquila Digital Community. For more information, please contact [Joshua.Cromwell@usm.edu](mailto:Joshua.Cromwell@usm.edu).

The University of Southern Mississippi

**Functionalizing  $\beta$ -Cyano Oligo(*p*-phenylene vinylene) Chromophores for use in  
Mechanochromic Materials**

by

Alexander Wink

A Thesis  
Submitted to the Honors College of  
The University of Southern Mississippi  
in Partial Fulfillment  
of the Requirements for the Degree of  
Bachelor of Science  
in the School of Polymers and High Performance Materials

May 2016



Approved by

---

Joseph R. Lott, Ph.D., Thesis Advisor  
Assistant Professor of Polymer Science  
and Engineering

---

Sarah E. Morgan, Ph.D., Interim Director  
School of Polymers and High Performance  
Materials

---

Ellen Weinauer, Ph.D., Dean  
Honors College

## Abstract

Mechanochromic materials are materials that change color upon mechanical deformation. This concept can be applied in areas of quality control, since the knowledge of damaged parts will easily be detected due to a color change in the material that has undergone deformation. Typically these types of materials are enabled by employing functional small molecules. Often, these are conjugated organic molecules or chromophores, which fluoresce different colors determined by the stimulus (or lack thereof) acting upon the material. In this work, we explore a new avenue to elicit color changes in polymeric materials based on the process of restriction of intramolecular rotations (RIR) phenomena in  $\beta$ -cyano oligo(*p*-phenylene vinylene) (cyano-OPVs) molecules. To develop the molecular structure-property relationships required for engineering stimuli-responsive polymers based on the cyano-OPV motif, this study systematically varied functional group placement and electronic characteristics on the cyano-OPV framework. A series of eight molecules was synthesized in which hydrogen, methyl, dimethyl, cyano, fluoro, and methoxy functionalities were placed onto the terminal phenyl rings. Structural characterization was accomplished using nuclear magnetic resonance (NMR) spectroscopy and the thermal characteristics of the molecules were measured by thermogravimetric analysis (TGA) and differential scanning calorimetry (DSC). The absorption spectra were recorded using UV-VIS spectroscopy and molar absorptivities of the chromophores were calculated based on the Beer-Lambert relationship. Finally, the RIR for these molecules was investigated with the use of photoluminescence measurements performed on both the pure solids as well as solutions of the cyano-OPVs.

Key Words: Mechanochromic, Oligo(phenylene vinylene), Stimuli Responsive Polymers

## **Acknowledgments**

I would like to thank my research advisor, Dr. Joseph Lott, for providing a productive and creative work environment for the graduate students, undergraduates, and me in his research lab. I've only been working with his research group for a year and a half, but in that short span of time I have learned so much. On top of providing an encouraging lab environment, Dr. Lott has also on many occasions provided insight on, for me, foreign concepts important to the research project. I cannot thank him enough for the patience and courtesy he has given me throughout the duration of the project. Working for him has allowed my love for the sciences to grow.

I would like to thank my graduate student, Brad Davis. He has been my main guide through the entirety of the project. From teaching a lab technique/process unfamiliar to me or giving advice on how to interpret data, Brad was there every step of the way. I am grateful to have worked with such a talented and hardworking scientist.

Finally, I would like to thank my parents for supporting me with their love and care (and shelter on weekends during stressful times), my brother for being a helpful consultant on science related matters, and my friends for being the motivation to keep going.

## Table of Contents

<b>List of Schemes, Figures, and Tables</b> .....	vii
<b>I. Introduction</b> .....	1
<b>II. Experimental Methods</b> .....	5
<b>III. Results</b> .....	12
<b>IV. Discussion</b> .....	21
<b>V. Conclusions</b> .....	24
<b>References</b> .....	25
<b>Appendices</b> .....	27

## List of Schemes, Figures, and Tables

### SCHEMES

**Scheme 1:** Synthesis of cyano-OPVs via Knoevenagel condensation.....6

### FIGURES

**Figure 1:** Cyano-OPV molecules investigated in this study.....6

**Figure 2:** Normalized absorption spectra of CHCl<sub>3</sub> solutions of dyes A through H .....14

**Figure 3:** Absorbance at  $\lambda_{\max}$  as a function of concentration for CHCl<sub>3</sub> solutions of dyes A through H.....16

**Figure 4:** Photoluminescence intensity as a function of wavelength from solid powders of dyes A through H. All spectra are normalized to maximum intensity of one except for (e).....18

**Figure 5:** Photoluminescence intensity as a function of wavelength for DMF solutions of dyes A through H .....20

### TABLES

**Table I:** Wavelength of absorption maxima ( $\lambda_{\max}$ ) for dyes A through H .....15

**Table II:** Extinction coefficients of dyes A through H.....17

**Table III:** Wavelength of maximum PL emission ( $\lambda_{\max}$ ) for dyes A through H in the solid state.....19



## **I. Introduction**

Stimuli responsive materials are a class of materials that allow different types of inputs or stimuli, such as thermal, chemical, electrical, mechanical, or optical inputs, to alter some material property of interest, i.e. obtain a desired response or output.<sup>1</sup> They provide a wealth of information when studying a particular system, such as smart polymers that can detect a temperature change, and add convenience to everyday life, such as touch-sensitive screens of smart phones or responsive capabilities of a DVD, which allow for data to be written or erased using beams of light. A class of stimuli responsive materials that has garnered attention in recent years is mechanochromic materials, which are materials that change colors after deformation due to some form of mechanical force.<sup>2</sup> Mechanochromic materials provide the ability for an observer to visually identify a mechanical perturbation in a studied system, while not changing the other material properties.

In past studies, the main components of mechanochromic materials are the chromophore and the polymer matrix that the chromophore inhabits.<sup>3</sup> The chromophore is what gives the mechanochromic material its color(s). The mechanism on how the chromophores display its color is due to the excitation of the electrons within the chromophore to a higher energy state after the chromophore has absorbed a photon, or a packet of energy. The subsequent relaxation of the excited molecule back down to the ground state results in the release of a photon, which is perceived by humans as color. This process is called fluorescence. A huge array of polymer matrices have been studied and proved to be an important aspect of the mechanochromic response in materials.<sup>4</sup> Particularly, the polymeric component determines the mechanical properties of the

material (flexibility vs. rigidity etc.) however, the polymer itself can display some type of stimuli response as well.<sup>5</sup>

The current work explores a new strategy to how chromophores can be used to create mechanochromic materials. This new approach manipulates a molecule's ability to relax from the excited electronic state via non-radiative (non-fluorescent) pathways. These processes have been previously observed in molecular systems, such as in twisted intramolecular charge-transfer (TICT) states<sup>6</sup> or restriction of intramolecular rotations (RIR).<sup>7</sup> Both behaviors relate to a molecule's ability to change conformation after its electrons are excited by an incident photon. This change in conformation opens a vibrational pathway that allows electrons in the excited state to relax to the ground state without fluorescing. Perturbing the balance between the two relaxation mechanisms (emissive and non-emissive) allows for the creation of a new type of "on" and "off" mechanochromic material. On the molecular level, this can be tailored by selection of functional groups on the chromophores that restrict or allow vibrational freedom through *intramolecular* steric interactions.

A particular class of chromophores that has been shown to be good candidates for these new mechanochromic materials are cyano-substituted oligo(*p*-phenylene vinylene) or cyano-OPVs.<sup>8-11</sup> In this study, various  $\beta$ -cyano OPVs are synthesized, and properties of the dyes, such as absorption, solid and liquid state fluorescence, and chemical structure are determined. Determining these properties will help allow us to understand the interplay between fluorescent emission and vibrational deactivation in this series of chromophores, which provides valuable information for designing future generations of mechanochromic sensors.

The inspiration of the work in investigating mechanochromic materials, along with other stimuli responsive materials, can be traced to observations made in nature. A notable example in this can be seen in animals such as the octopus and the chameleon, whose color change is a response to the ambient temperature surrounding the animal or the intensity of the light that strikes the animal's skin.<sup>12</sup> This change in color is due to chromatophores and iridophores, which are cells that are located under the reptile's/octopus's skin. The color changes are a result of the cells' mechanism that occur underneath the skin, which are basically the movement of muscles to make the pigments in the reptile's skin more prominent (chromatophores) or the diffraction of light within stacked transparent cells (iridophores).

In past studies, mechanically responsive materials may be obtained through two different routes: either a responsive molecular species being strongly bonded to a polymer chain through covalent bond or a responsive species introduced into a polymeric matrix and being dispersed throughout the matrix. In the latter case, those materials are generally obtained by properly combining chemical functional species, such as cyano OPVs (which are commonly referred to in the literature as "dyes"), into a multiphase system (polymer composite or matrix) whose response can be effectively changed, in terms of intensity and selectivity, by controlling the interaction between the two components.<sup>12</sup>

The color switching mechanism is a result of changes in conformation or intermolecular interactions of the dye attached to, or dispersed in polymer. The works of Christoph Weder have shown the color switching properties of mechanochromic polymers. Weder and colleagues dispersed small amounts (0.01-3 wt%) of excimer-

forming OPV chromophore into a ductile polymer matrix (e.g. linear low density polyethylene, LLDPE).<sup>13</sup> When deformation is applied to film, the chains in polymer orient themselves and, as a result, break up the dye aggregates. This causes a color change, which is depicted via plot of photoluminescent (PL) intensity by wavelength.<sup>14</sup> The film before deformation displays a color at a wavelength around 650 nanometers (nm) in the form of a peak and after deformation this peak in the graph disappears, with the prominent peak in the material's spectra being at around 500 nm, which corresponds to a green color. This change in emission properties is easily noticeable, from orange-red excimers, which is excited dimers,<sup>15</sup> to molecularly dissolved green monomers. Color change is directly related to the monomer-to-excimer ratio, which increases with progressive film drawing.<sup>14</sup>

There have been papers published that discussed different functionalities added to cyano OPVs, in particular alkyl chains attached to the molecule as end groups.<sup>14,16</sup> In the research done by Weder and Lott, they were able to functionalize a cyano OPV with differing alkyl chains as end groups and test the mechanochromic properties by monitoring emission during deformation of polymer films.<sup>14</sup>

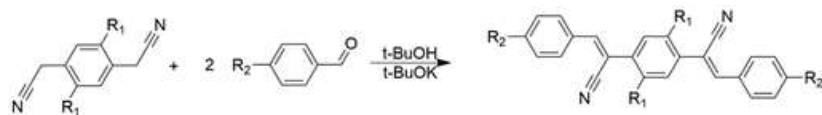
The lengths of the alkyl chain end groups tested were one carbon and 18 carbons, with the designated names C1-RG and C18-RG, respectively. Aggregation of dyes and how this aggregation of dyes separate is important for the emission color changes in the polymer. The differing alkyl tails changed solubility of the chromophores in the polymer matrix, leading to a change in aggregation properties which, as stated previously, is important for the color changes in the mechanochromic material. The dyes must have the ability to self-assemble in the polymer matrix in order to give a particular color to the

material. Upon deformation, aggregates are broken up, which leads to color change. Another thing to consider when including dye into polymer matrix is the concentration of the dyes, since they influence the size of the aggregates.<sup>14</sup> The size of the aggregates need to be small enough in order to disperse when deformed. Better dispersion properties can be achieved when smaller aggregates are formed.

The work dealing with chromophores and polymeric matrices was novel ideas at the time, around 2002, in the world of mechanochromic materials, and has provided a good starting point in that area. However, there is a different approach on how these chromophores are able to fluoresce, and it can be done through the manipulation of a molecule's ability to adopt a TICT or RIR state. These states stem from the molecule's ability to move its electrons around itself and between its substituents, an electron donor and an electron acceptor.<sup>6</sup> During absorption, an electron is excited from its ground state orbital into an excited state orbital. The excited electron can return to the ground state by non-emissive means, e.g. releasing heat through vibrations, or by emissive means, via fluorescence.<sup>6,7</sup> If a balance between the two methods of relaxation can be achieved in a molecule, a new class of stimuli responsive material can be made by placing them into materials that can manipulate the molecule's vibrational freedom.

## II. Experimental Methods

The objective of this project is to synthesize a library of chromophores in the use of mechanochromic materials and characterize the synthesized products in order to determine their optical properties. **Scheme 1** displays the general reaction scheme for the synthesis of the chromophore.



**Scheme 1:** Synthesis of cyano-OPVs via Knoevenagel condensation.

The R groups, R<sub>1</sub> and R<sub>2</sub>, indicate a location where functional groups can be added to the reagent in order to give particular properties to the final product, such as solubility in aqueous or organic medium, high melting point, or color. However, this study will focus on placing electron donating or withdrawing groups at various locations on the two peripheral rings. The selected synthetic targets are presented in Figure 1.

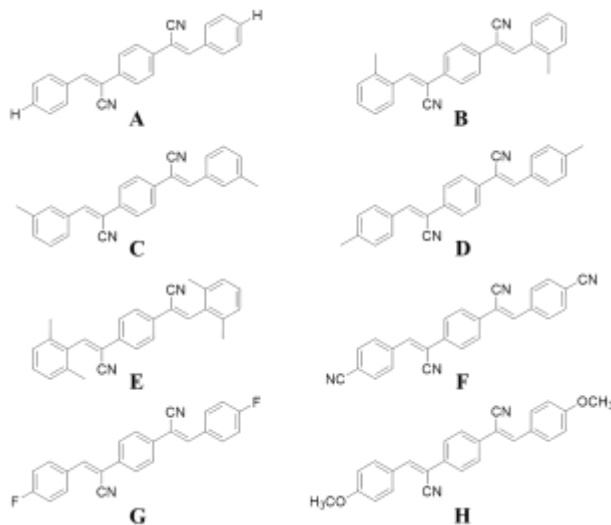


**Figure 1:** Cyano-OPV molecules investigated in this study.

### Materials

All of the solvents used in this project were purchased from Fischer Chemicals. 1,4-phenylene diacetonitrile and 2,6-dimethylbenzaldehyde were purchased from Alfa Aesar. *Tert*-butoxide and the remaining functionalized aldehydes were purchased from Acros Organics. All chemicals were used as received without further purification.

### Instrumentation

An Agilent Cary 500 UV-VIS-NIR spectrometer was used to obtain UV-Vis spectra of dyes G (4-fluoro-β-cyano OPV) and B (*o*-methyl-β-cyano OPV), and a

PerkinElmer Lambda 35 UV-VIS spectrometer was used to obtain the absorption spectra of the remaining dyes. Thermogravimetric analysis (TGA) was performed using a TA Instruments TGA Q<sub>500</sub> under an N<sub>2</sub>(g) atmosphere with a heating rate of 15 °C/min. DSC was carried out using a TA Instruments DSC Q100 under N<sub>2</sub>(g) atmosphere and heating rate of 15 °C/min. NMR spectrum for dyes C, D, E, and H were obtained by a Varian Mercury 300 MHz NMR spectrometer. Solid and solution state photoluminescence spectrum for the dyes were obtained using an OceanOptics Flame-S-VIS-NIR-ES spectrometer.

#### *Synthesis of H-β-cyan-OPV (dye A)*

1,4-phenylene diacetonitrile (1.000 g, 6.21 x 10<sup>-3</sup> mol), *tert*-butanol (111.8 mL), tetrahydrofuran (37.28 mL), and benzaldehyde (1.344 mL, 1.317 x 10<sup>-2</sup> mol) were added to a 3-neck round bottom flask and allowed to homogenize at 35°C. *Tert*-butoxide (1.0 M in THF, 13.66 mL, 1.366 x 10<sup>-2</sup> mol) was added, dropwise, and the reagents reacted for an hour. The reaction was allowed to cool to room temperature and quenched by pouring methanol (300 mL) containing glacial acetic acid (15 drops). This mixture was stored overnight in freezer in order to promote complete precipitation of the product. The crude product was isolated using vacuum filtration, and the collected solid was copiously washed with cold methanol. The solid crude product was dried *in vacuo* (40°C, -27 in Hg) overnight to remove residual solvent. The crude product (890.7 mg) was recrystallized from 1-butanol (400 mL). The final product was obtained after being dried *in vacuo* overnight (43.15 % yield). The compound was a light yellow solid powder.

#### *Synthesis of o-methyl-β-cyano-OPV (dye B)*

1,4-phenylene diacetonitrile (0.2000 g, 1.242 x 10<sup>-3</sup> mol), *tert*-butanol (22.81mL),

tetrahydrofuran (7.604 mL), and *o*-tolualdehyde (0.3200 mL,  $2.712 \times 10^{-3}$  mol) were added to a 3-neck round bottom flask and allowed to homogenize at 35°C. *Tert*-butoxide (1.0 M in THF, 2.732 mL,  $2.733 \times 10^{-3}$  mol) was added, dropwise, and the reagents reacted for an hour. The reaction was allowed to cool to room temperature and quenched by pouring methanol (300 mL) containing glacial acetic acid (2 drops). This mixture was stored overnight in freezer in order to promote complete precipitation of the product. The crude product was isolated using vacuum filtration, and the collected solid was copiously washed with cold methanol. The solid crude product was dried *in vacuo* (40°C, -27 in Hg) overnight to remove residual solvent. The crude product (388.0 mg) was recrystallized from 1-butanol (700 mL). The final product was obtained after being dried *in vacuo* overnight (86.74 % yield). The compound was a light brown solid powder.

*Synthesis of m-methyl-β-cyano-OPV (dye C)*

1,4-phenylene diacetonitrile (0.2000 g,  $1.242 \times 10^{-3}$  mol), *tert*-butanol (22.81 mL), tetrahydrofuran (7.604 mL), and *m*-tolualdehyde (0.3200 mL,  $2.712 \times 10^{-3}$  mol) were added to a 3-neck round bottom flask and allowed to homogenize at 35°C. *Tert*-butoxide (1.0 M in THF, 2.732 mL,  $2.733 \times 10^{-3}$  mol) was added, dropwise, and the reagents reacted for an hour. The reaction was allowed to cool to room temperature and quenched by pouring methanol (300 mL) containing glacial acetic acid (2 drops). This mixture was stored overnight in freezer in order to promote complete precipitation of the product. The crude product was isolated using vacuum filtration, and the collected solid was copiously washed with cold methanol. The solid crude product was dried *in vacuo* (40°C, -27 in Hg) overnight to remove residual solvent. The crude product (102.4 mg) was recrystallized from 1-butanol (70 mL). The compound was dissolved in minimal amounts



of chloroform and passed through a small plug of silica (50 mm diameter, 40 mm height). The final product was obtained after rotary evaporation, and dried *in vacuo* overnight. The compound was a bright, yellow solid powder.

*Synthesis of p-methyl-β-cyano-OPV (dye D)*

1,4-phenylene diacetonitrile (0.296 g,  $1.342 \times 10^{-3}$  mol), *tert*-butanol (34.50 mL), tetrahydrofuran (12.00 mL), and *p*-tolualdehyde (0.5000 mL,  $2.912 \times 10^{-3}$  mol) were added to a 3-neck round bottom flask and allowed to homogenize at 35°C. *Tert*-butoxide (1.0 M in THF, 4.310 mL,  $3.133 \times 10^{-3}$  mol) was added, dropwise, and the reagents reacted for an hour. The reaction was allowed to cool to room temperature and quenched by pouring methanol (300 mL) containing glacial acetic acid (2 drops). This mixture was stored overnight in freezer in order to promote complete precipitation of the product. The crude product was isolated using vacuum filtration, and the collected solid was copiously washed with cold methanol. The solid crude product was dried *in vacuo* (40°C, -27 in Hg) overnight to remove residual solvent. The crude product (291.0 mg) was recrystallized from 1-butanol (200 mL). The final product was obtained after being dried *in vacuo* overnight (43.03 % yield). The compound was a bright yellow solid powder.

*Synthesis of 2,6-dimethyl-β-cyano-OPV (dye E)*

1,4-phenylene diacetonitrile (0.2000 g,  $1.242 \times 10^{-3}$  mol), *tert*-butanol (22.81 mL), tetrahydrofuran (7.604 mL), and 2,6-dimethyl benzaldehyde (0.3666 mL,  $2.740 \times 10^{-3}$  mol) were added to a 3-neck round bottom flask and allowed to homogenize at 35°C. *Tert*-butoxide (1.0 M in THF, 2.732 mL,  $2.658 \times 10^{-3}$  mol) was added, dropwise, and the reagents reacted for an hour. The reaction was allowed to cool to room temperature and quenched by pouring methanol (300 mL) containing glacial acetic acid (2 drops). This

mixture was stored overnight in freezer in order to promote complete precipitation of the product. The crude product was isolated using vacuum filtration, and the collected solid was copiously washed with cold methanol. The solid crude product was dried *in vacuo* (40°C, -27 in Hg) overnight to remove residual solvent. The crude product (270.0 mg) was recrystallized from 1-butanol (100 mL). The final product was obtained after being dried *in vacuo* overnight (58.41 % yield). The compound was a light, greyish-brown solid powder.

#### *Synthesis of 4-cyano-β-cyano-OPV (dye F)*

1,4-phenylene diacetonitrile (0.2000 g,  $1.242 \times 10^{-3}$  mol), *tert*-butanol (22.81 mL), tetrahydrofuran (7.604 mL), and 4-cyano-benzaldehyde (0.3557 g,  $2.712 \times 10^{-3}$  mol) were added to a 3-neck round bottom flask and allowed to homogenize at 35°C. *Tert*-butoxide (1.0 M in THF, 2.732 mL,  $2.733 \times 10^{-3}$  mol) was added, dropwise, and the reagents reacted for an hour. The reaction was allowed to cool to room temperature and quenched by pouring methanol (300 mL) containing glacial acetic acid (2 drops). This mixture was stored overnight in freezer in order to promote complete precipitation of the product. The crude product was isolated using vacuum filtration, and the collected solid was copiously washed with cold methanol. The solid crude product was dried *in vacuo* (40°C, -27 in Hg) overnight to remove residual solvent. The crude product (380.1 mg) was recrystallized from 1-butanol (430 mL). The final product was obtained after being dried *in vacuo* overnight (80.02 % yield). The compound was a brownish orange solid powder.

#### *Synthesis of 4-fluoro-β-cyano-OPV (dye G)*

1,4-phenylene diacetonitrile (0.2000 g,  $1.242 \times 10^{-3}$  mol), *tert*-butanol (22.81 mL), tetrahydrofuran (7.604 mL), and 4-fluoro-benzaldehyde (0.2904 mL,  $2.712 \times 10^{-3}$  mol)

were added to a 3-neck round bottom flask and allowed to homogenize at 35°C. *Tert*-butoxide (1.0 M in THF, 2.732 mL,  $2.733 \times 10^{-3}$  mol) was added, dropwise, and the reagents reacted for an hour. The reaction was allowed to cool to room temperature and quenched by pouring methanol (300 mL) containing glacial acetic acid (2 drops). This mixture was stored overnight in freezer in order to promote complete precipitation of the product. The crude product was isolated using vacuum filtration, and the collected solid was copiously washed with cold methanol. The solid crude product was dried *in vacuo* (40°C, -27 in Hg) overnight to remove residual solvent. The crude product (378.0 mg) was recrystallized from 1-butanol (450 mL). The final product was obtained after being dried *in vacuo* overnight (82.89 % yield). The compound was a bright yellow solid powder.

*Synthesis of 4-methoxy-β-cyano-OPV (dye H)*

1,4-phenylene diacetonitrile (2.000 g,  $1.240 \times 10^{-2}$  mol), *tert*-butanol (228.2 mL), tetrahydrofuran (76.00 mL), and 4-methoxybenzaldehyde (3.294 mL,  $2.712 \times 10^{-2}$  mol) were added to a 3-neck round bottom flask and allowed to homogenize at 35°C. *Tert*-butoxide (1.0 M in THF, 27.33 mL,  $2.730 \times 10^{-2}$  mol) was added, dropwise, and the reagents reacted for an hour. The reaction was allowed to cool to room temperature and quenched by pouring methanol (500 mL) containing glacial acetic acid (4 drops). This mixture was stored overnight in freezer in order to promote complete precipitation of the product. The crude product was isolated using vacuum filtration, and the collected solid was copiously washed with cold methanol. The solid crude product was dried *in vacuo* (40°C, -27 in Hg) overnight to remove residual solvent. The crude product (3.7112 g) was

recrystallized from 1-butanol (500 mL). The final product was obtained after being dried *in vacuo* overnight (76.22 % yield). The compound was a bright yellow solid powder.

### III. Results

The analogues of the  $\beta$ -cyano OPV chosen for this project are based on the influence different substituent groups have on both electronic and *intramolecular* sterics. These factors will control the molecule's chemical and electronic properties, such as melting temperature, solubility, ability to fluoresce in solid or solution, and changes in wavelengths at which the dye absorbs and fluoresces. The unsubstituted  $\beta$ -cyano OPV, dye A, was synthesized as a reference molecule in order to compare the differences in the aforementioned properties of the non-functionalized dyes to the functionalized analogues. This molecule contains no electron withdrawing or donating groups on the peripheral rings and therefore will have the least "push-pull" effect as well as minimal steric interactions. Dyes B, C and D were functionalized with weakly electron donating methyl groups in different positions (*ortho*, *meta*, *para*) on the terminal phenyl rings of the molecule in order to evaluate their effect on the optical properties. Dye E, contains methyl functionalities at both the 2 and 6 positions on the terminal rings. At these positions, the methyl groups can be expected to sterically interact with the central phenyl ring of the cyano-OPV. Dyes F and G have strongly electron withdrawing groups while dye H has the strongly donating methoxy groups attached to the *-para* position of peripheral rings. Taken together, the collection of dyes examined in the current study provides a platform to discern the interplay between electronic and steric effects in cyano-OPVS.

These dyes were all synthesized via Knoevenagel condensation<sup>17</sup> with readily available starting materials and provided adequate yield of the product. Structural confirmation was accomplished with the use of <sup>1</sup>H-NMR spectroscopy (Appendix A). However, several of the molecules (Dyes A, B, F, G) had very low solubility in organic solvents. As a result, solutions with sufficient concentrations for <sup>1</sup>H-NMR experiments could not be prepared, even with the application of heat and sonication. Therefore, <sup>1</sup>H-NMR confirmation of the chemical structures of these dyes was not performed. However, based on the optical characteristics of these molecules, it is highly likely the desired structures were successfully synthesized. In the future, solid state <sup>1</sup>H-NMR experiments may provide a method to obtain appropriate spectra for thorough characterization. Lastly, for all molecules synthesized, TGA (Appendix B) was used to analyze the thermal degradation.

The energy of photons absorbed by a molecule is a result of the electric effects that alter the energy gap between the highest occupied molecular orbital (HOMO) and the lowest unoccupied molecular orbital (LUMO) levels, as well as the conjugation length of the molecule. Molecules with significant push-pull character via interaction between electron donating and withdrawing groups will display lower energy (red shifted) absorbance spectra.<sup>18</sup> Additionally, red shifting of absorbance spectra is also induced by increasing the conjugation length. Therefore, absorbance measurements can directly probe the HOMO-LUMO energetic differences. UV-VIS spectra were recorded for chloroform (CHCl<sub>3</sub>) solutions at sufficiently dilute concentration to preclude any aggregation of the dyes. The results from these measurements are presented in Figure 2.

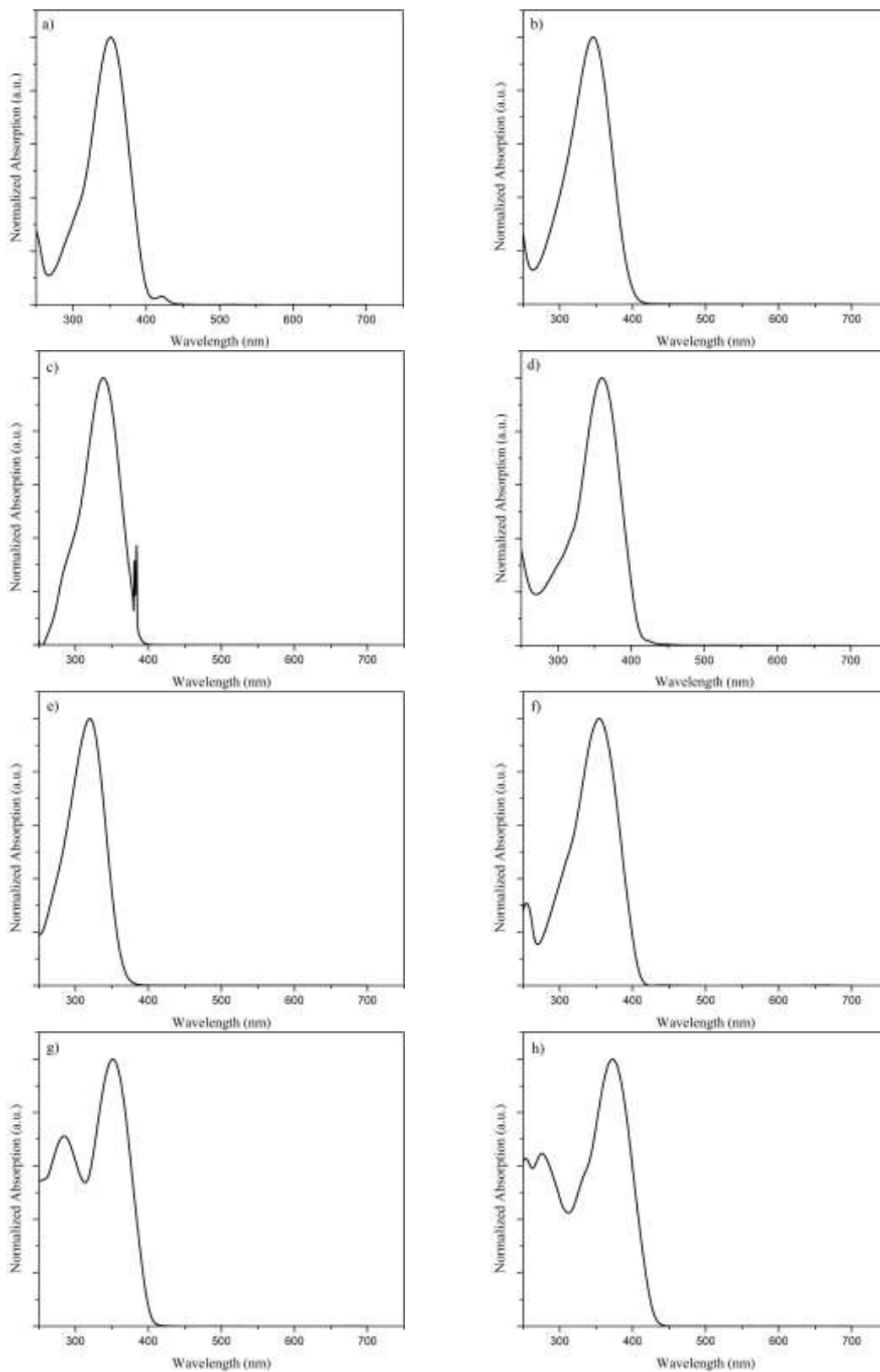


**Figure 2:** Normalized absorption spectra of  $\text{CHCl}_3$  solutions of dyes A through H.

The wavelengths of maximum absorbance for each dye are tabulated in Table I. Dye H, substituted with an electron donating group, has its primary absorption at the highest wavelength, 371 nm, of all the dyes. Dye G, substituted with an electron withdrawing group, has a lower  $\lambda_{\text{max}}$  than Dye H, but higher than the methyl substituted dyes (dyes B through E). Dye E, which is substituted with two methyl groups in the *ortho* position, has significantly lower  $\lambda_{\text{max}}$  than the other analogues.

**Table I:** Wavelength of absorption maxima ( $\lambda_{\text{max}}$ ) for dyes A through H.

Dye	A	B	C	D	E	F	G	H
$\lambda_{\text{max}}$ (nm)	352	347	338	359	320	354	351	371

The magnitude of a particular sample's absorbance ( $A$ ) depends on the path length through which the beam travels through the sample ( $b$ ), the molar concentration of the absorbing species ( $c$ ), the molar absorptivity ( $\epsilon$ ) or extinction coefficient of the molecule as described by the Beer-Lambert law:

$$A = \epsilon bc \quad (1)$$

Equation 1 can be used to quantify the extinction coefficient of a molecule by measuring absorbance as a function of concentration. The resulting extinction coefficients will provide a method in future materials, to precisely determine the amount of dye in a given polymeric material. Using chloroform as a solvent, serial dilutions were employed to prepare solutions of varying concentration and the UV-VIS spectra were measured. Figure 3 contains the absorbance at  $\lambda_{\text{max}}$  for each dye as a function of concentration. The data was fit with a linear regression and the slope of the trend line provides the extinction coefficients.

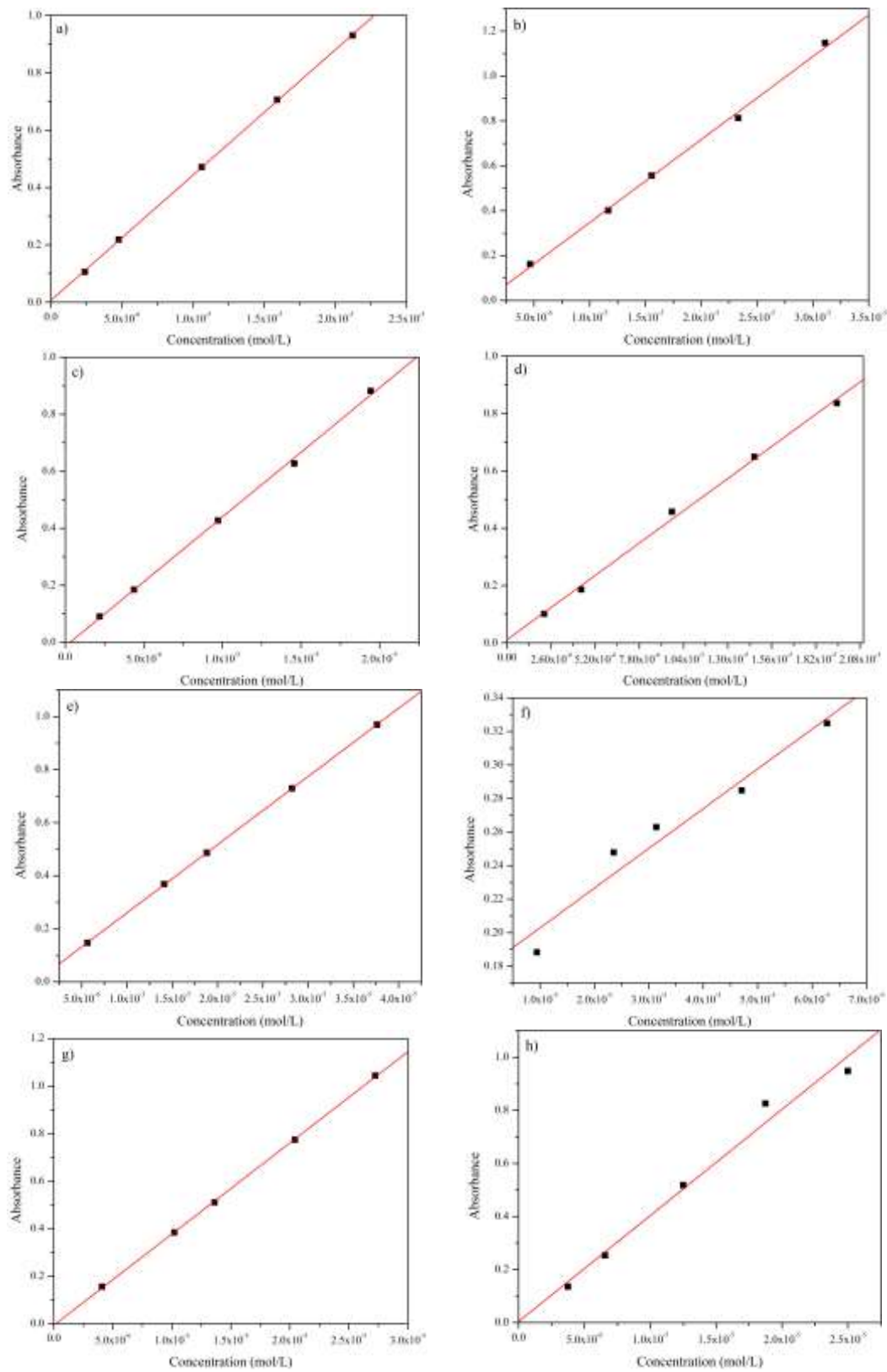


**Figure 3:** Absorbance at  $\lambda_{\max}$  as a function of concentration for  $\text{CHCl}_3$  solutions of dyes A through H.



The data presented in Figure 3 clearly portray the linear relationship predicted by equation 1, and the fits resulted in  $R^2$  values ranging from 0.98-1.0. From the Beers-Lambert plots, the extinction coefficients, the strength at which a molecule absorbs a particular wavelength, of the dyes were extrapolated from the slope of the linear best fit line. These values are listed in Table II.

**Table II:** Extinction coefficients of dyes A through H.

Dye	A	B	C	D	E	F	G	H
$\epsilon$ ( $L \cdot mol^{-1} \cdot cm^{-1}$ )	43,751	36,962	45,328	43,195	25,695	2368	38,376	39,993

The emissive properties of the molecules are captured by measuring the energy (or wavelength) of photons released after the absorption process. The stimuli response of the cyano-OPVs is based on the notion that when vibrations are hindered, the molecules fluoresce. In the solid powders of the dyes, molecular stacking occurs and prevents vibrational deactivation of the emission. For example, under excitation from a UV lamp (365 nm) the as-synthesized solids typically display intense fluorescence. Photoluminescence (PL) intensity was measured as a function of wavelength for each of dyes studied. In order to observe emission, one must ensure that the excitation wavelength corresponds to one that is absorbed by the molecule. For the PL experiments, an excitation wavelength of 385 nm was typically used. However, for dye E, this wavelength is not absorbed, therefore 325 nm light was used for this molecule. The results from these experiments are shown in Figure 4.

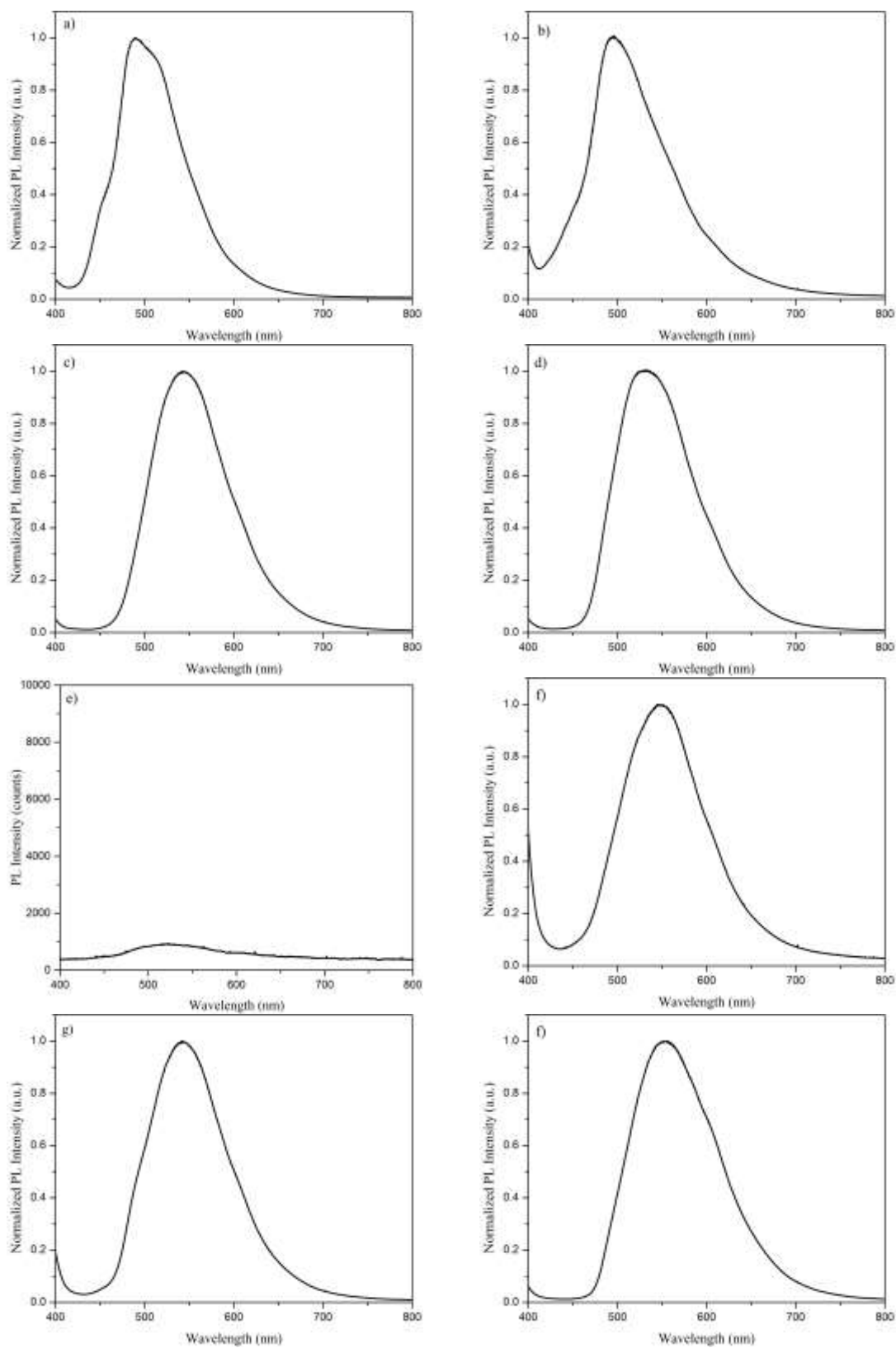


**Figure 4:** Photoluminescence intensity as a function of wavelength from solid powders of dyes A through H. All spectra are normalized to maximum intensity of one except for (e).

All molecules except for dye E were highly fluorescent and the data was normalized to a peak intensity of one. Unexpectedly, dye E exhibited very weak emission and the data was depicted using actual photon counts to portray the weak emission. The molecules emit over a range of  $\sim 490 - 550$  nm, which is consistent with emission from the excimer state.<sup>8</sup> The wavelengths at which maximum emission is observed are tabulated in Table III.

**Table III:** Wavelength of maximum PL emission ( $\lambda_{\text{max}}$ ) for dyes A through H in the solid state.

Dye	A	B	C	D	E	F	G	H
$\lambda_{\text{max}}$ (nm)	489	493	542	534	523	548	543	556

As opposed to the solid powders, the solution state provides an environment in which the molecules are free to vibrate. Based on the RIR notion, this will allow for non-emissive pathways for relaxation from excited electronic states. To verify this behavior in the collection of dyes studied, similar PL studies were conducted in dimethylformamide (DMF) solutions. In all cases, the same excitation wavelengths were used in these experiments as were for the solid state PL measurements. As expected, in solution, all of the dyes displayed little to no fluorescence (Figure 5). Weak emission is observed for dyes D and F. It is likely that these dyes aggregated during testing due to solubility issues, giving rise to the observed emission. This notion is further supported by the wavelengths at which the emission occurs, which is similar to what is observed in Figure 4 for the solid powders.

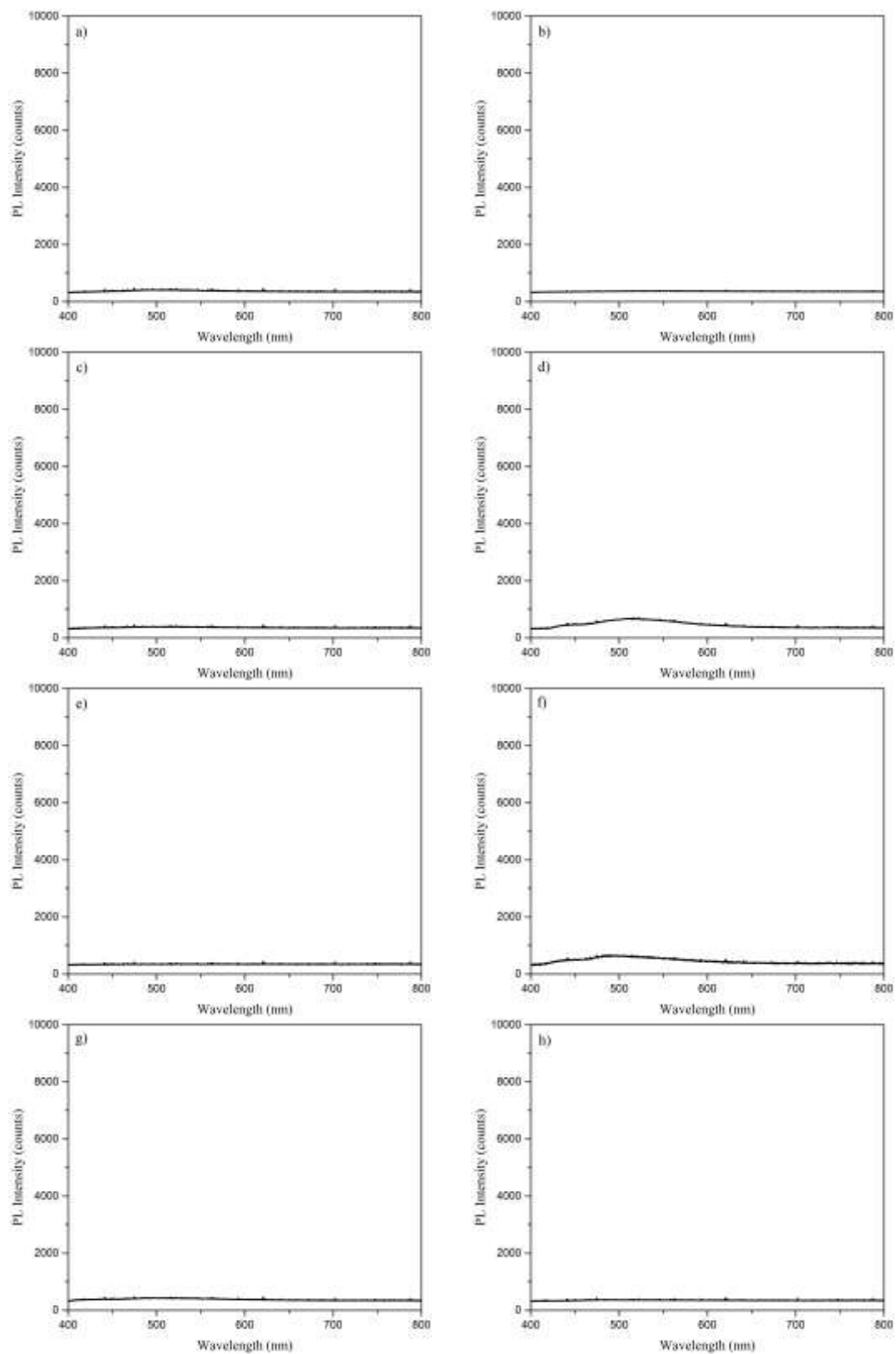


**Figure 5:** Photoluminescence intensity as a function of wavelength for DMF solutions of dyes A through H.

## IV. Discussion

For the cyano-OPVs in this investigation, there are two forces that are believed to play a role in the way the dyes absorb light at a given wavelength: the electronic (the push-pull effect) and/or the steric effects of the substituents. The chemical identity of the substituents dictates the electronic properties, while the location of the substituents on the peripheral rings influences the amount of steric interaction with the central ring or vinyl linkage. The absence of any groups on Dye A minimizes both electronic and steric effects and therefore makes it useful for comparison with the functionalized dyes. The simplest comparison is using Dye D, which contains a weakly electron donating methyl group attached to outer phenyl rings in the *para*- position. This position of the weakly donating group keeps it spatially removed from the core of the molecule and minimizes the steric influence. A weak push-pull effect is responsible for the slight redshift of the absorbance maximum versus dye A (359 vs 352 nm).

Dyes B and C are also functionalized with methyl groups, but in the *ortho*- and *meta*- positions respectively. These positions allow for steric interactions with other portions of the molecule. The absorbance data shows the maxima are both blue shifted in comparison to dye A. Dye B has the methyl group in the *ortho* position, which is in conjugation with the aromatic cyano-OPV. This will allow electronic contributions from the donating methyl group. Therefore, one might expect a similar  $\lambda_{\text{max}}$  for dye B and D. However, dye B is blue shifted by over 10 nm compared to D. This discrepancy can only be explained by an opposing steric interaction; the methyl group in the *ortho* position causes a distortion from planarity and effectively shortens the conjugation length. For dye C, the steric effect overshadows the electronic push-pull contribution. Dye C has a

methyl group at the *-meta* position, which is not in conjugation with the delocalized system and therefore there is no push-pull character to redshift the absorbance. Therefore, the blue shift in absorbance can be attributed to steric twisting leading to decreased conjugation length. It is interesting to note that even at the *-meta* position, the methyl groups apparently interact with the center core on the cyano-OPV.

Dye E is similar in structure to B, however has two methyl groups as opposed to one. Electronically, this will increase the push-pull character. However, this molecule displays the lowest wavelength absorption of all those examined. Therefore, a drastic decrease in conjugation length must be present to dominate over the effect of electron donating and withdrawing groups. Examining the structure, it is presumed that the two methyl groups force the molecule to adopt a highly twisted conformation to minimize steric interactions between the methyl groups and the cyano group and/or center portion of the dye.

Dyes F and G have little difference in wavelength of maximum absorption compared to dye A. F and G have electron withdrawing groups as substituents on the terminal rings as well as vinyl linkage. With only withdrawing groups, there is no push-pull effect in the molecule. Steric hindrance is bypassed since the substituents are well removed from the center ring. These two factors combined contribute to F and G's little difference in wavelength of maximum absorption.

Dye H displays the lowest energy absorption of all the dyes, which can be understood by the electronic effects the 4-methoxy group provides to the molecule. Similar to *-para* methyl, the 4-methoxy is an electron donating group, contributing to the push-pull effect of the molecule. However, 4-methoxy is a much stronger electron

donating group than methyl, which gives rise to a higher wavelength of maximum absorption.

The well-established ability of cyano-OPVs to form excimer complexes was also observed in the molecules examined within this study. For all molecules except for dye E, the solid powders were highly emissive. Dye E exhibited a very low fluorescence quantum yield. Currently, it is not known why the emission from this molecule was so weak. This molecule contains intramolecular steric interactions caused by the two *ortho*-methyl groups on the tail end of the molecule. We hypothesize that these groups may lock the molecule into a conformation that inhibits the  $\beta$ -cyano OPV from fluorescing. Further studies such as x-ray scattering to determine solid state structure and PL lifetime measurements to explore the possible formation of triplet excited states should be explored to fully understand this behavior.

In solution, the dyes experienced displayed PL activity that is orders of magnitude lower than the solid powders. This supports the idea that the molecules' ability to vibrate, which is enhanced in solution, inhibits the dyes' ability to fluoresce. This occurred for all of the dyes, indicating that functionality of the dyes plays little role in fluorescing capabilities in solution. Further insight could be gained by freezing these solutions into the solid state. In these samples, the solid solvent should inhibit the vibrational ability and PL should be observed from the single molecules that is distinctly different than from the excimer complexes.

## V. Conclusions

The  $\beta$ -cyano-OPVs considered in this study continue to display a more diverse range of behavior than the  $\alpha$ -cyano-OPV isomers that fluoresce in all scenarios. The molecule absorbance wavelength can be easily tuned with the appropriate balance of electron donating and withdrawing groups along with strategically placing the groups at locations that promote or avoid steric interactions. The elucidation of role of sterics into the optical properties of the molecules represents new insight into this family of chromophores. Most interestingly, the current work uncovered a novel cyano-OPV (dye E) that displays very little emission in the solid state. Further studies on this phenomenon could lead to expanded strategies towards realizing stimuli responsive polymers based on the cyano-OPV motif. Taken together, the work contained herein provides valuable structure property relationships that can inform future generations on mechanochromic polymers based on the novel mechanism of restriction of molecular vibrations.



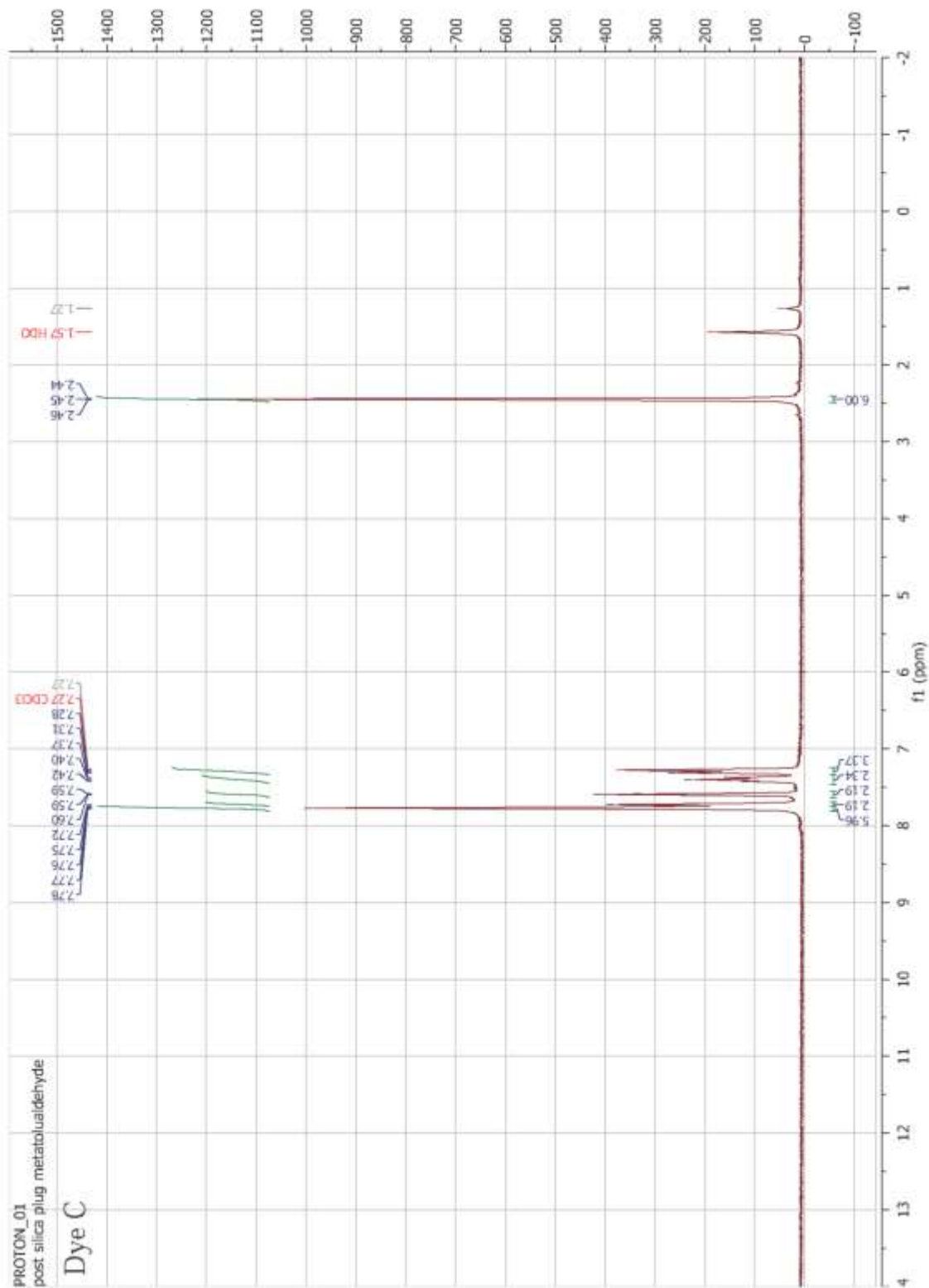
## References

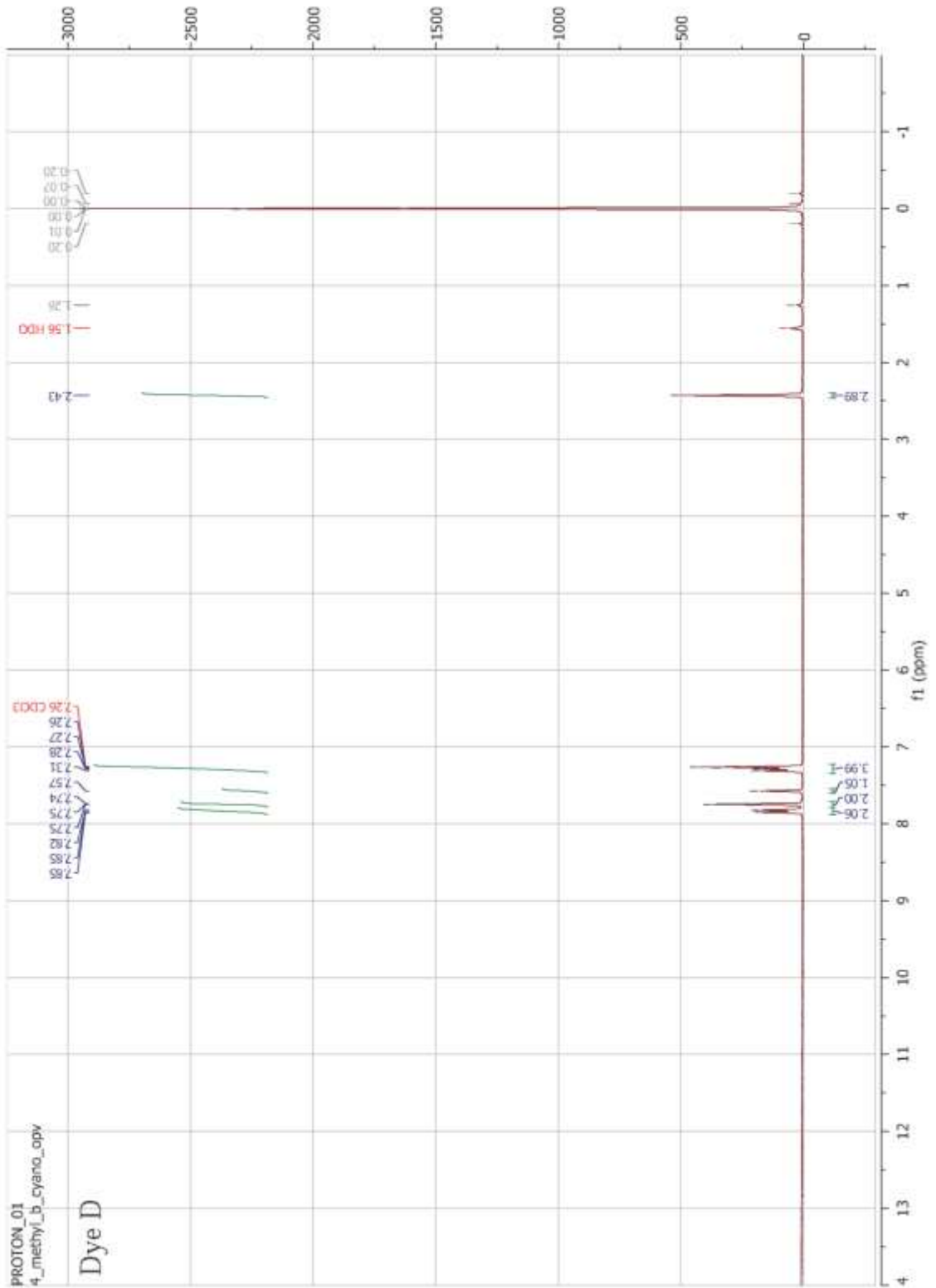
1. Guragain, S.; Bastakoti, B.P.; Malgras, V.; Nakashima, K.; Yamauchi, Y. *European Journal of Chemistry*. **2015**, *21*, 13164.
2. Wiggins, K. M.; Brantley, J. N.; Bielawski, C. W. *Chemical Society Reviews*. **2013**, *42*, 7130.
3. Ciardelli, F.; Ruggeri, G.; Pucci, A. *Chemical Society Reviews*. **2013**, *42*, 857.
4. Roberts, D. R. T.; Holder, S. J. *Journal Material Chemistry*. **2011**, *21*, 8256.
5. Kunzleman, J.; Chung, T.; Mather, P. T.; Weder, C. *Journal Material Chemistry*. **2008**, *18*, 1082.
6. Grabowski, Z.R., Rotkiewicz, K., Rettig, W. *Chemical Reviews*., **2003**, *103*, 3899.
7. Hong, Y.; Lam, J. W. Y.; Tang, B. Z. *Chemical Society Reviews*. **2011**, *40*, 5361.
8. Löwe, C.; Weder, C. *Advance Materials*. **2002**, *14*, 1629.
9. Li, Y.; Li, F.; Zhang, H.; Xie, Z.; Xie, W.; Xu, H.; Li, B.; Shen, F.; Ye, L.; Hanif, M.; Ma, D.; Ma, Y. *Chemical Communications*. **2007**, *3*, 231.
10. Lott, J.; Ryan, C.; Valle, B.; Johnson, J. R.; Schiraldi, D. A.; Shan, J.; Singer, K. D.; Weder, C. *Advance Materials*. **2011**, *23* , 2425.
11. An, B.-K.; Gierschner, J.; Park, S. Y. *Accounts of Chemical Reseach*. **2012**, *45*, 544.
12. Pucci, A.; Bizzarri, R.; Ruggeri, G. *Soft Matter*. **2011**, *7*, 3689.
13. Weder, C.; Crenshaw B.R. *Chemistry of Materials*. **2003**, *15*, 4717.
14. Lott, J.; Weder, C. *Macromolecular Chemistry and Physics*. **2010**, *211*, 28.
15. Birks, JB. *Reports on Progress in Physics*. **1975**, *38*, 903.
16. Makowski, B. T.; Lott, J.; Valle, B.; Singer, K. D.; Weder, C. *Journal of Materials Chemistry*. **2012**, *22*, 5190.

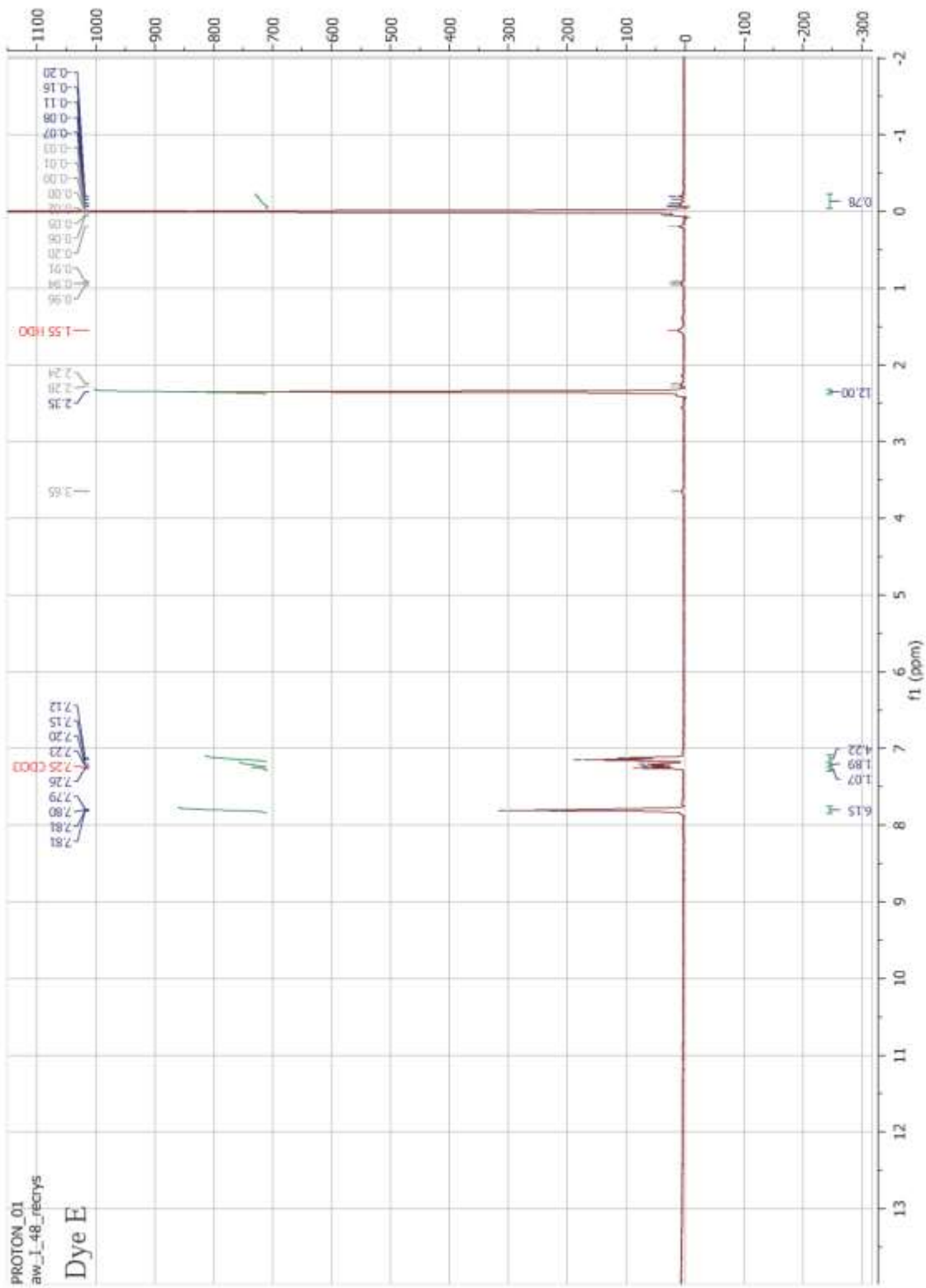
17. Gill, R. E.; van Hutten, P. F.; Meetsma, A.; Hadziioannou, G. *Chemistry of Materials*. **1996**, *8*, 1341.
18. Bureš, F. *Royal Society of Chemistry Advances*. **2014**, *4*, 58826.

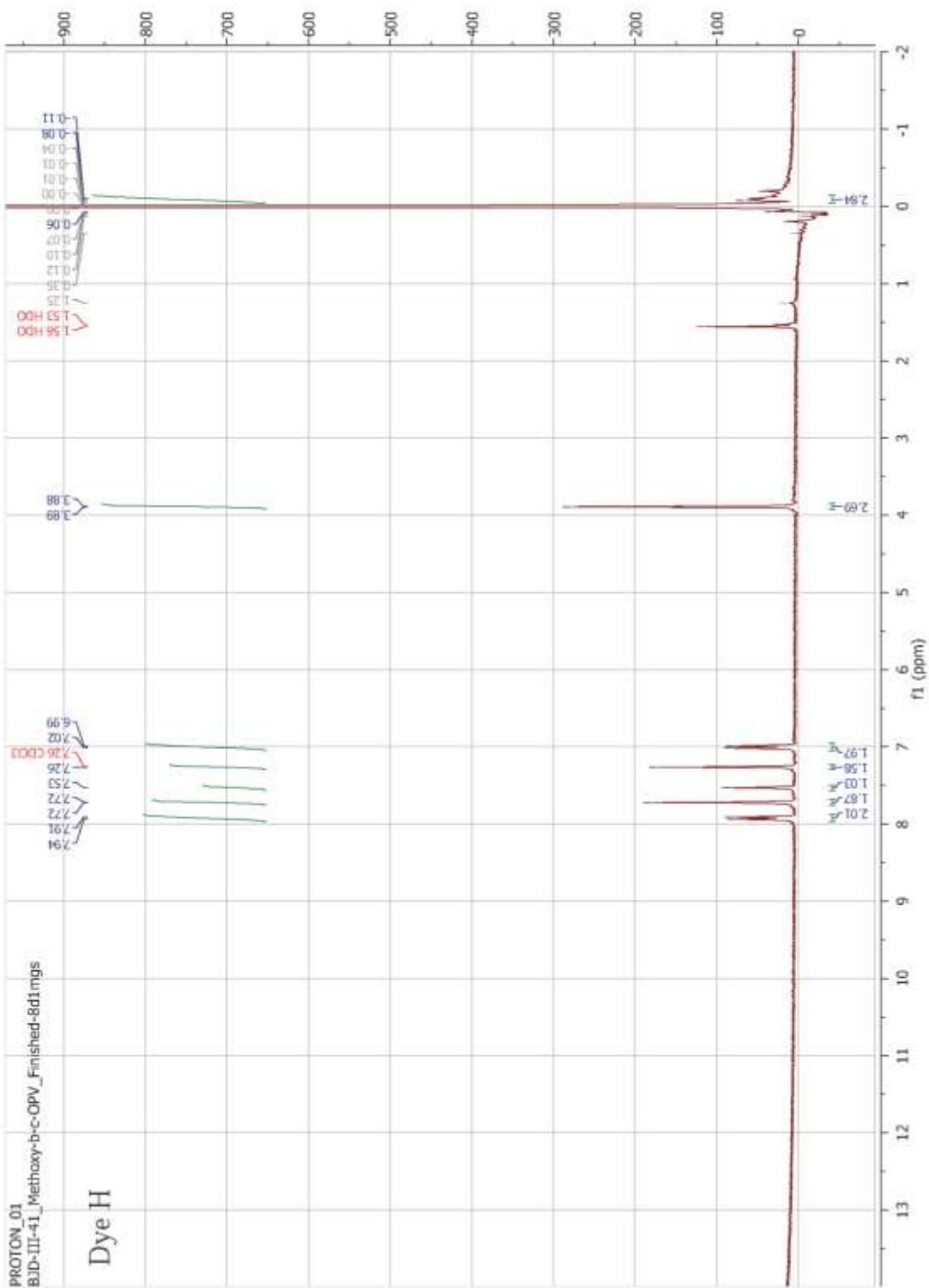
# Appendices

Appendix A:  $^1\text{H}$  Nuclear magnetic resonance spectra recorded in  $\text{CDCl}_3$ .

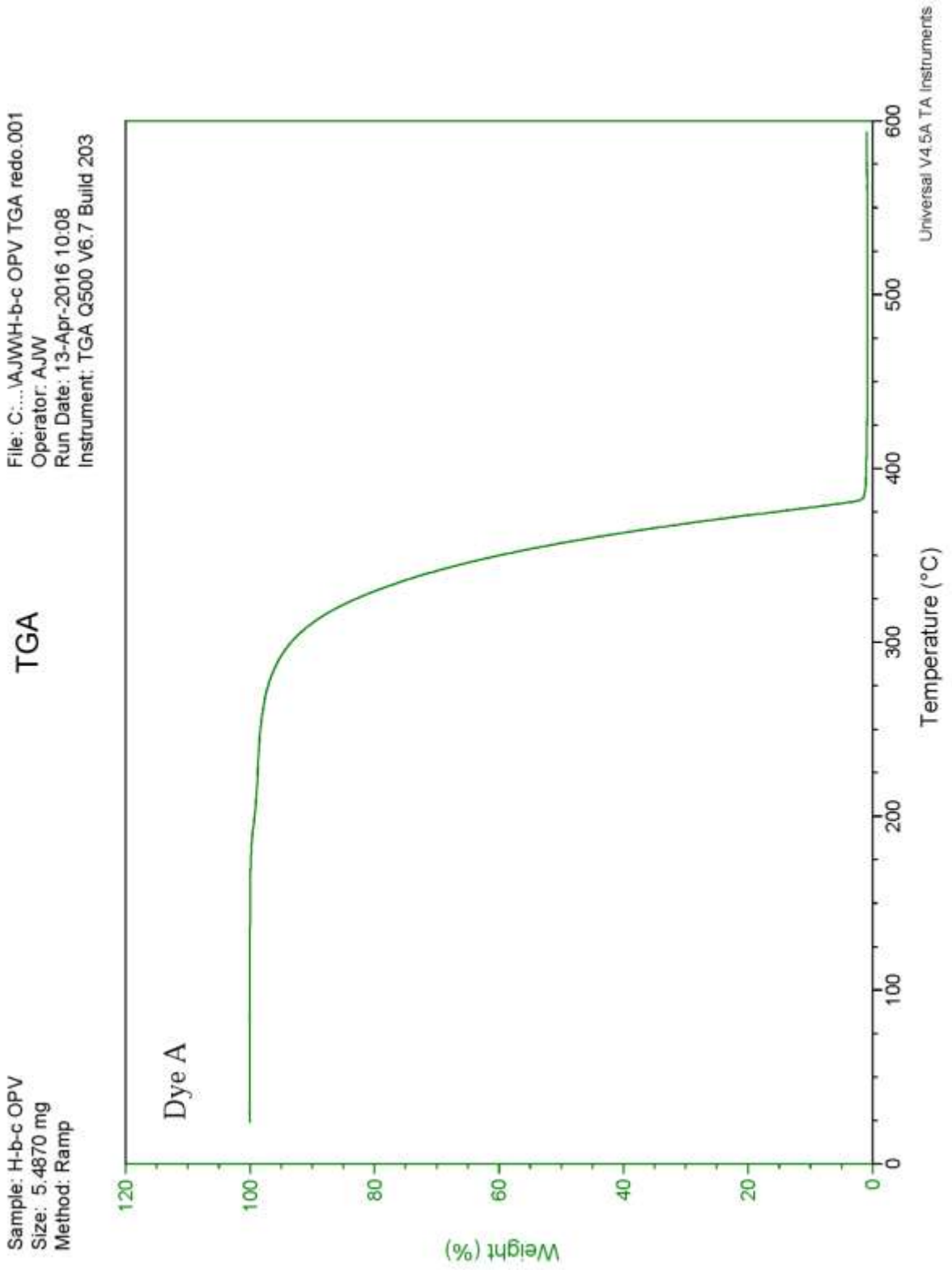








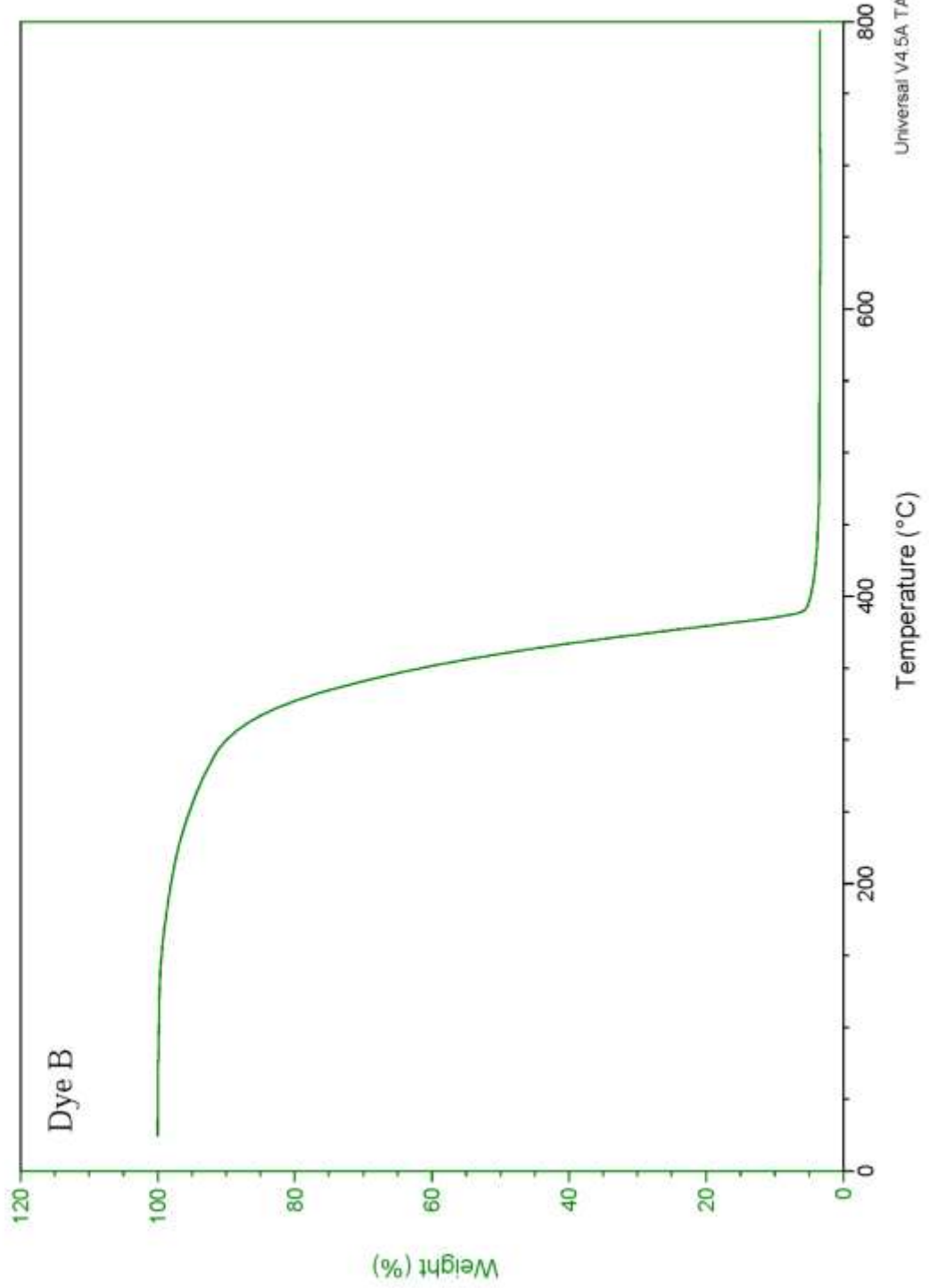
**Appendix B:** Thermogravimetric analysis of dyes A through H.



Sample: AW-I-27  
Size: 7.6910 mg  
Method: Ramp

## TGA

File: C:\...\TGA\AW-I-27 TGA.001  
Operator: AJW  
Run Date: 24-Mar-2016 14:17  
Instrument: TGA Q500 V6.7 Build 203



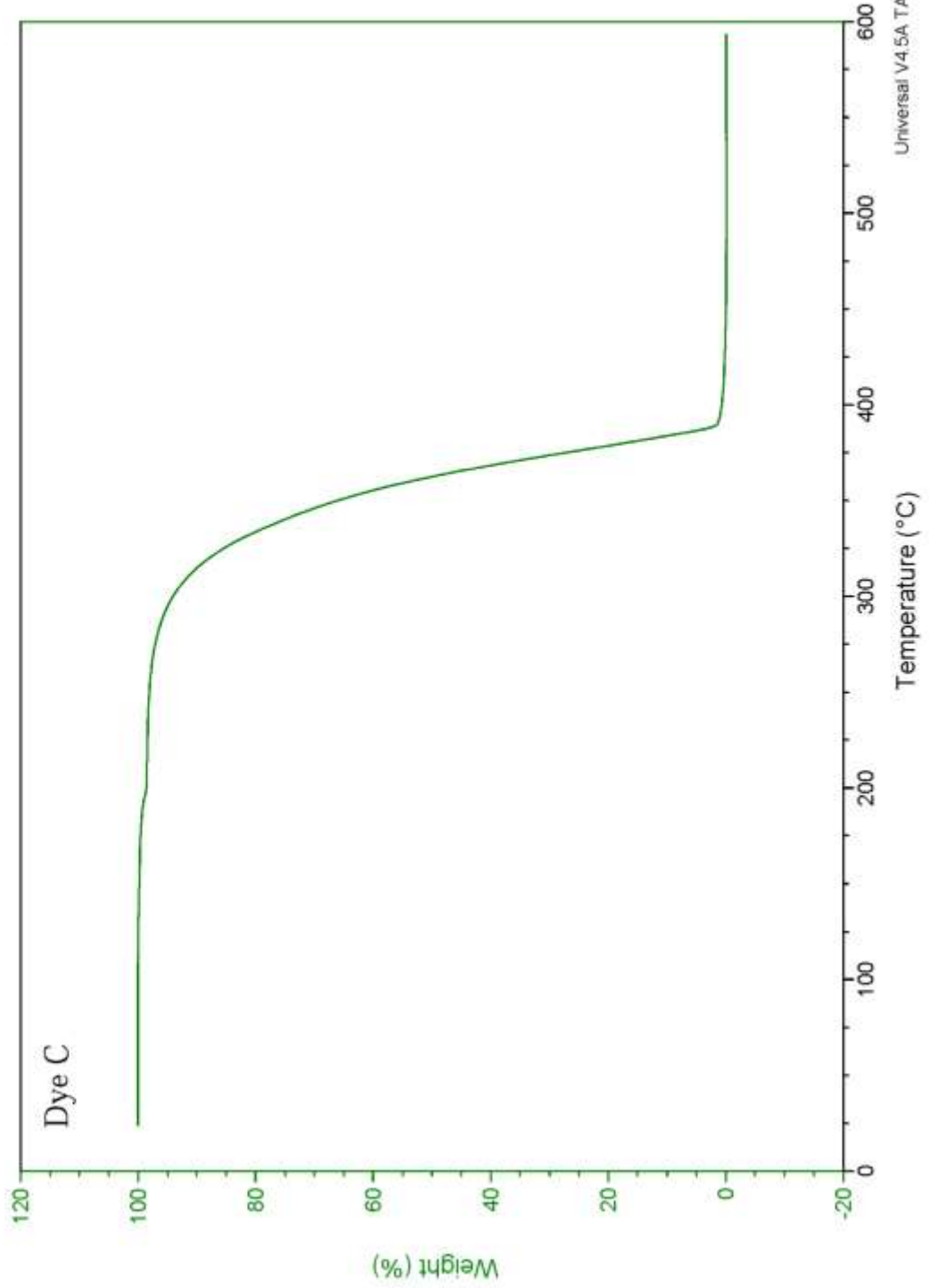
Universal V4.5A TA Instruments



Sample: aw-l-23  
Size: 4.8520 mg  
Method: Ramp

## TGA

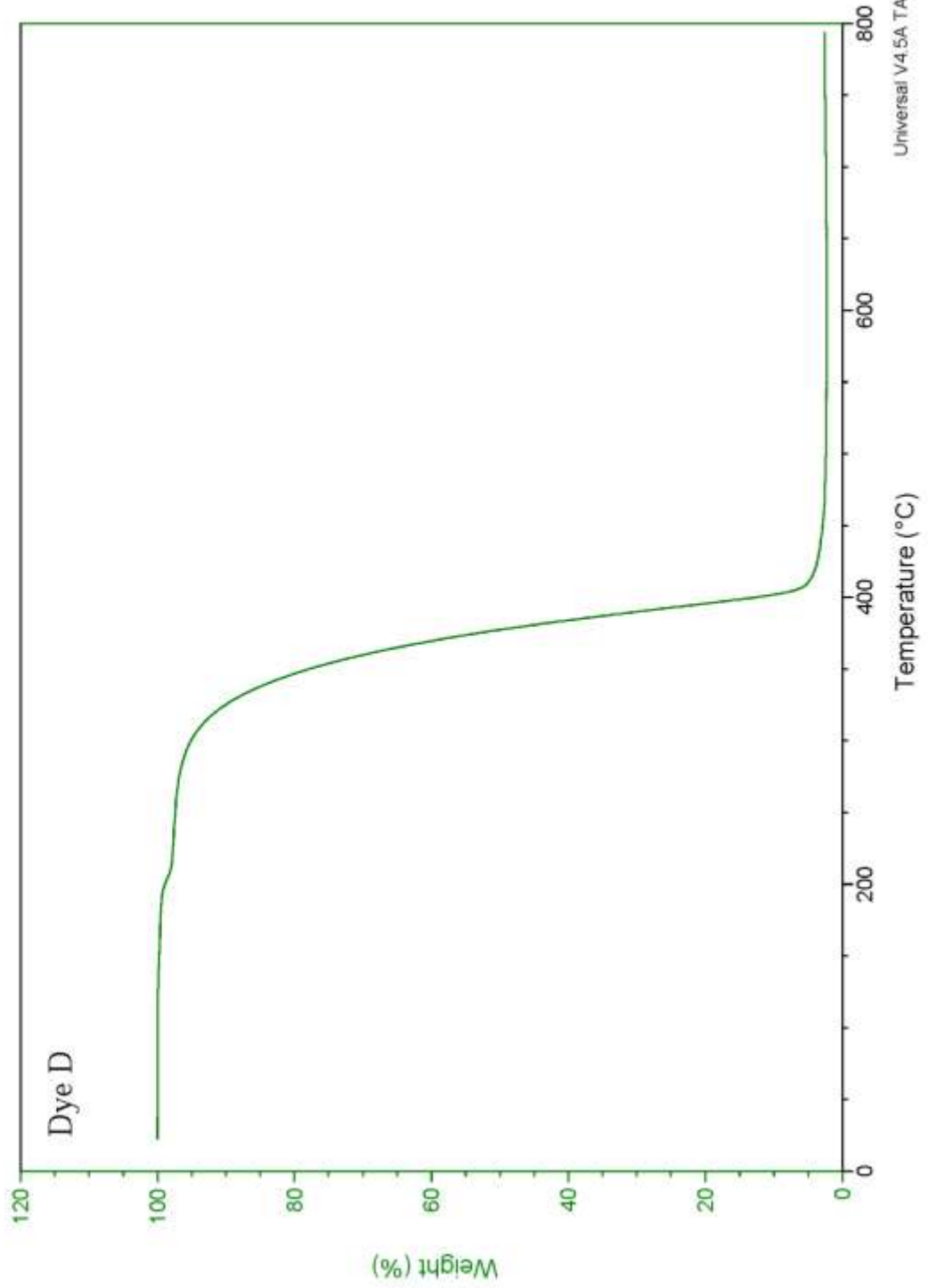
File: C:\... \TGA\m-methyl-b-c OPV TGA.001  
Operator: AJW  
Run Date: 10-Apr-2016 21:24  
Instrument: TGA Q500 V6.7 Build 203



Sample: 4-methyl-b-c OPV  
Size: 5.8590 mg  
Method: Ramp

### TGA

File: C:\...4-methyl-b-c OPV TGA.001  
Operator: AJW  
Run Date: 03-Apr-2016 11:20  
Instrument: TGA Q500 V6.7 Build 203

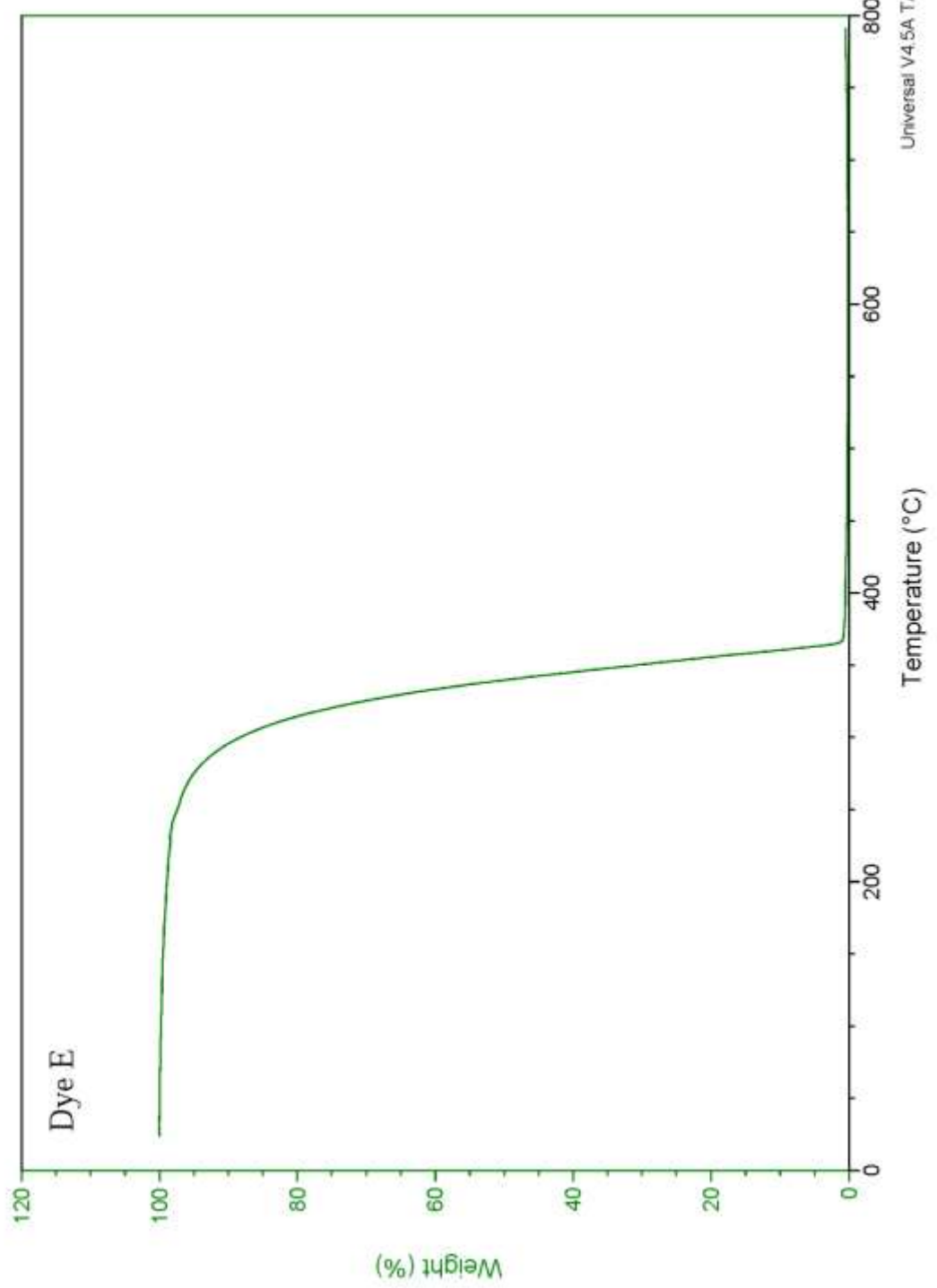


Universal V4.5A TA Instruments

File: C:\... \TGA\AW-I-48.001  
Operator: AW  
Run Date: 01-Mar-2016 11:35  
Instrument: TGA Q500 V6.7 Build 203

### TGA

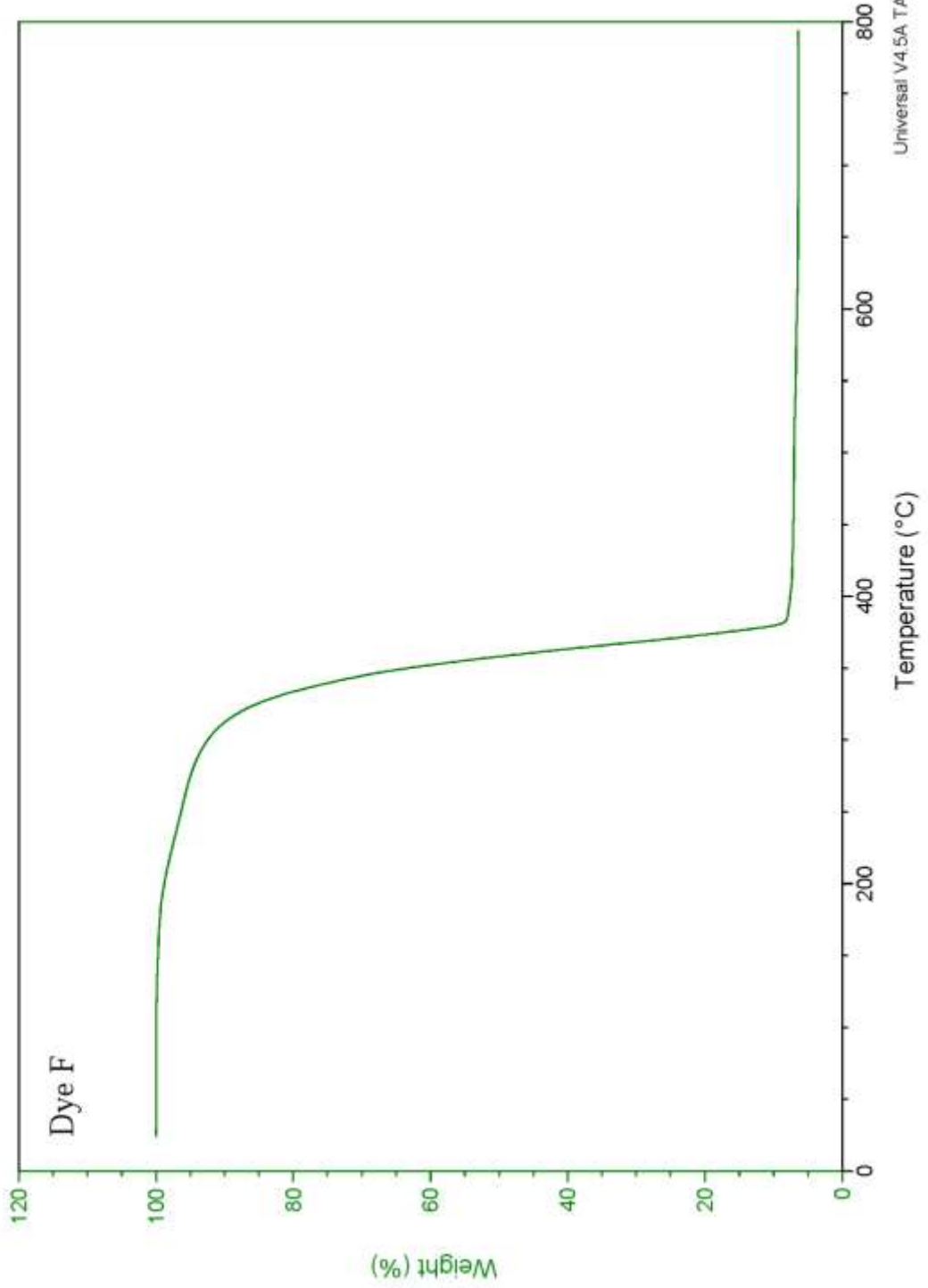
Sample: AW-I-48  
Size: 2.9150 mg  
Method: Ramp  
Comment: 2,6-dimethyl-b-c-OPV



Sample: AW-I-41  
Size: 6.5120 mg  
Method: Ramp

### TGA

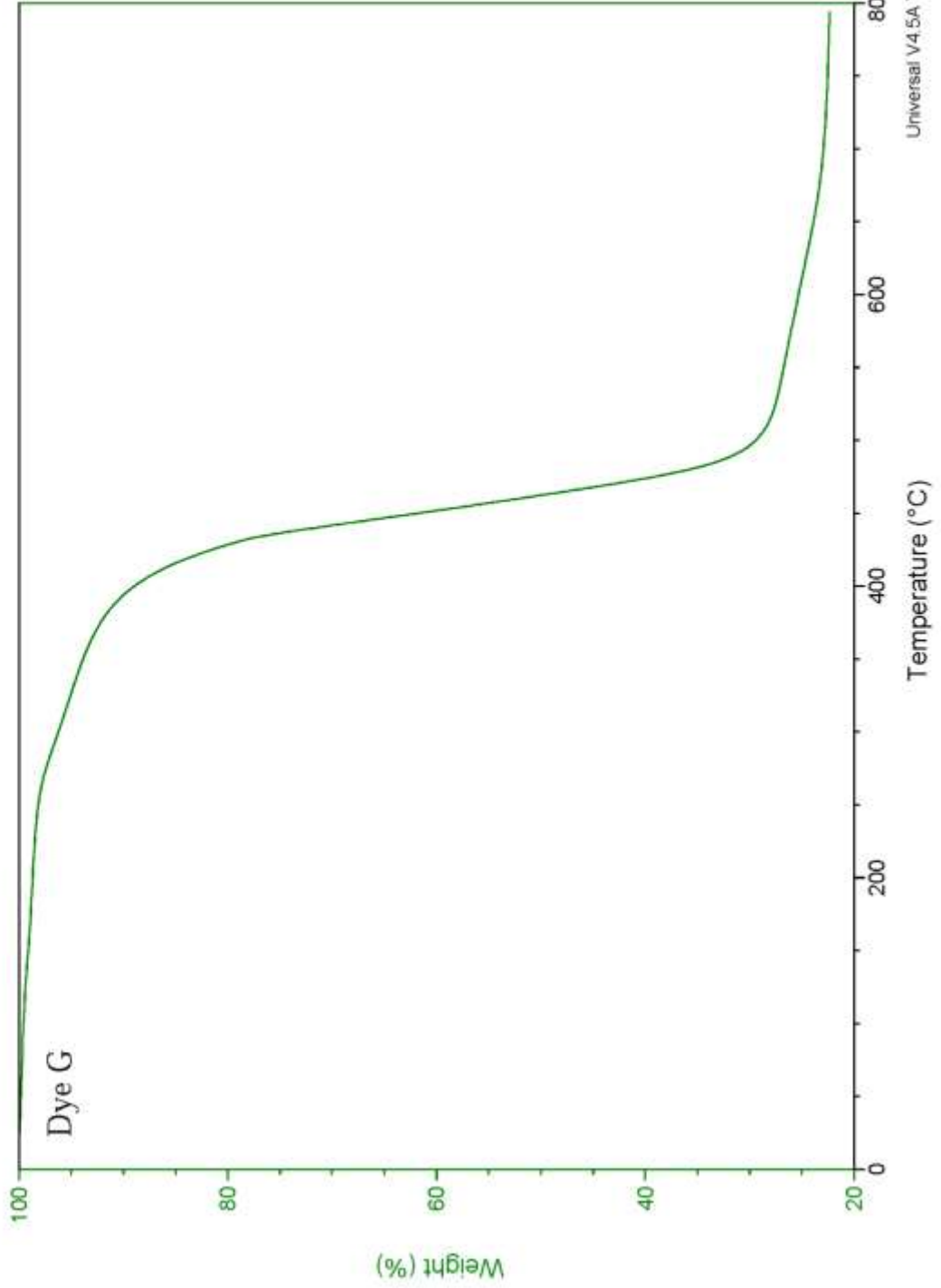
File: C:\...\TGA\AW-I-41 TGA.001  
Operator: AJW  
Run Date: 24-Mar-2016 11:27  
Instrument: TGA Q500 V6.7 Build 203



Sample: AW-I-37  
Size: 13.0240 mg  
Method: Ramp

### TGA

File: C:\...\TGA\AW-I-37 TGA.002  
Operator: AJW  
Run Date: 28-Mar-2016 10:23  
Instrument: TGA Q500 V6.7 Build 203

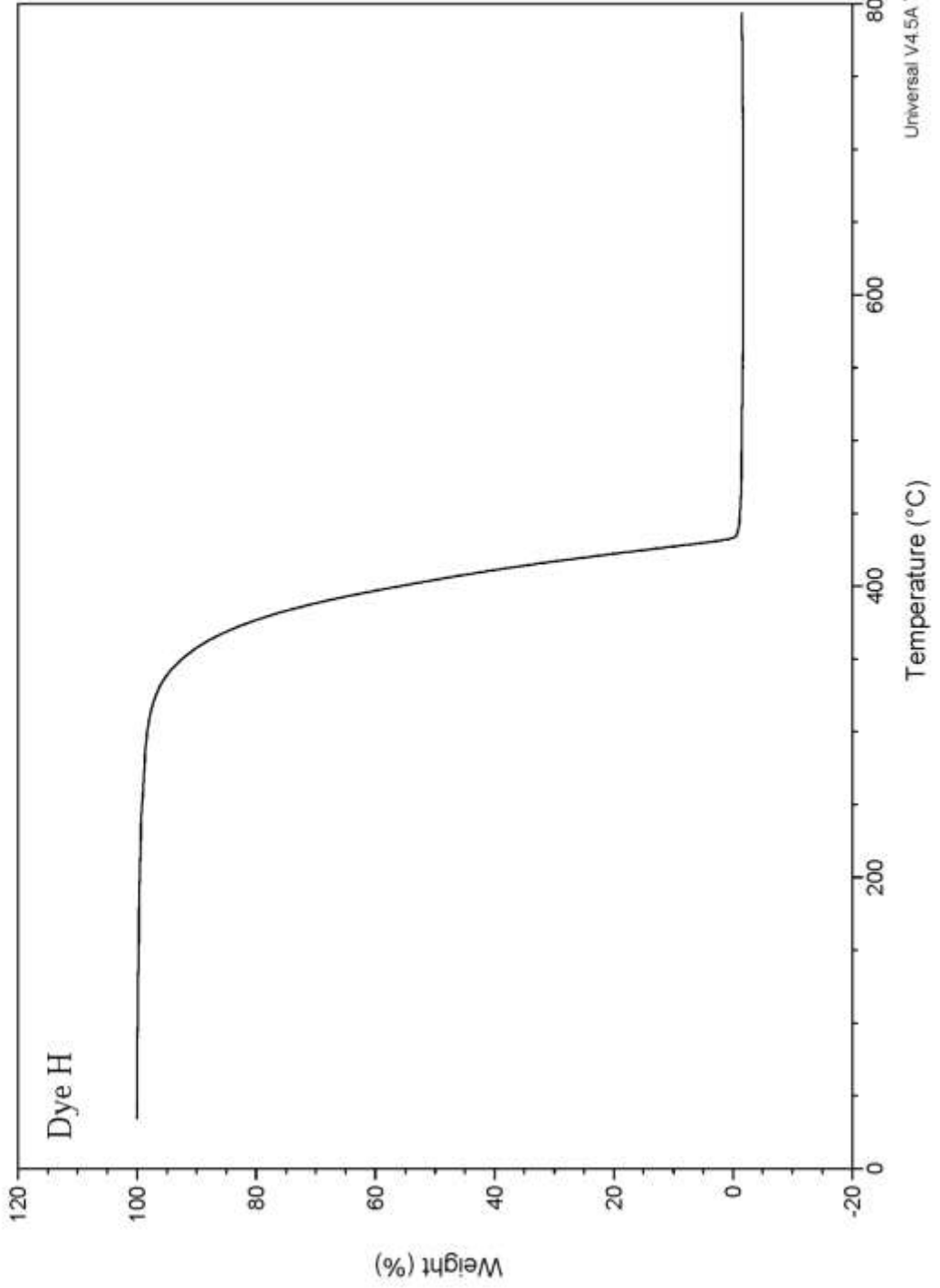


Universal V4.5A TA Instruments

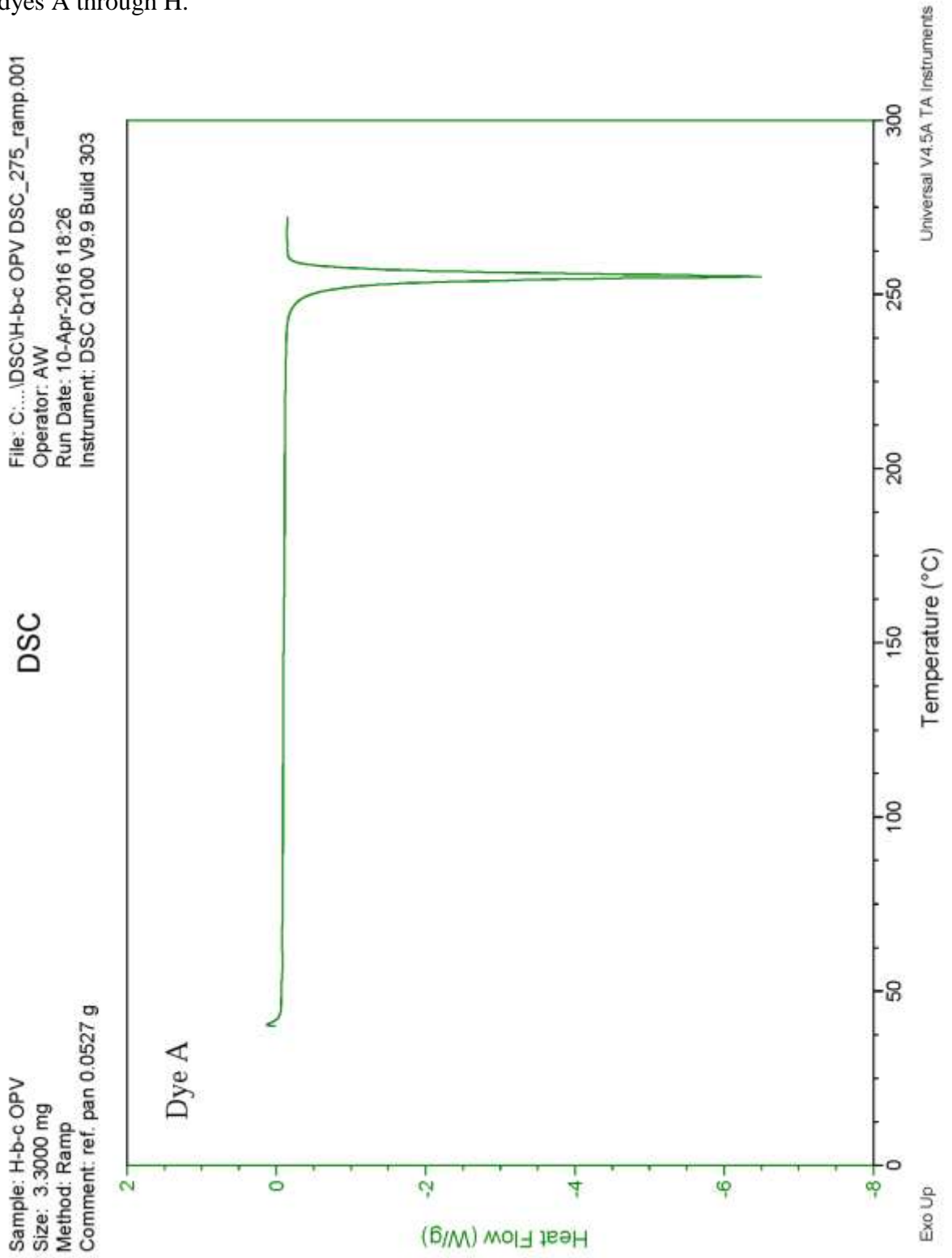
Sample: methoxy-b-c-OPV  
Size: 4.8440 mg  
Method: Ramp  
Comment: Methoxy ramp

### TGA

File: C:\...\BJD-III-41\_methoxy.0021  
Operator: bjd  
Run Date: 17-Mar-2016 09:57  
Instrument: TGA Q500 V6.7 Build 203



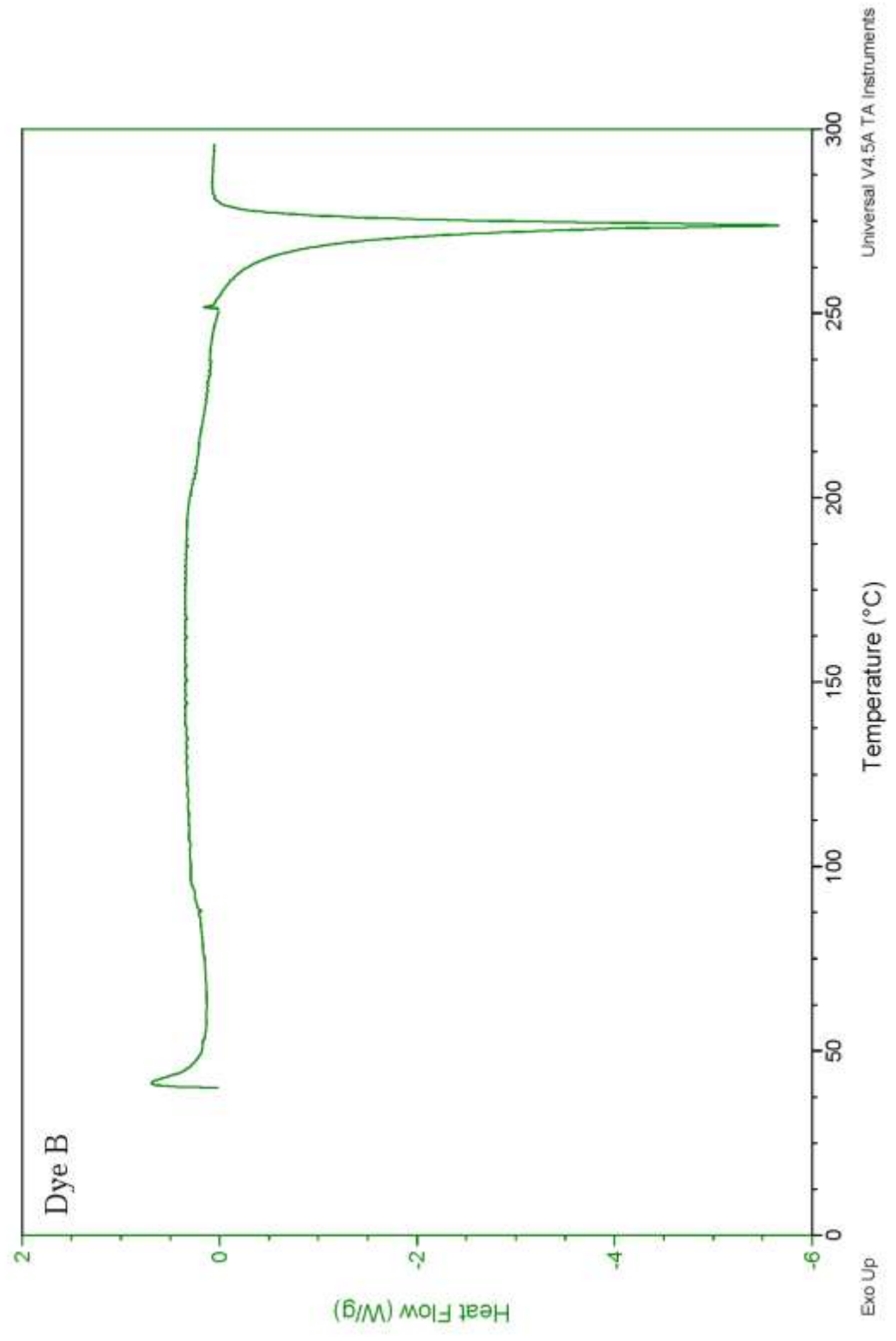
**Appendix C:** Differential scanning calorimetry (first heating curves) thermograms of dyes A through H.



Sample: ortho-methyl-b-c OPV  
Size: 2.1000 mg  
Method: Ramp

### DSC

File: C:\...lo-methyl-b-c OPV DSC\_300\_ramp.002  
Operator: AW  
Run Date: 26-Apr-2016 11:13  
Instrument: DSC Q100 V9.9 Build 303



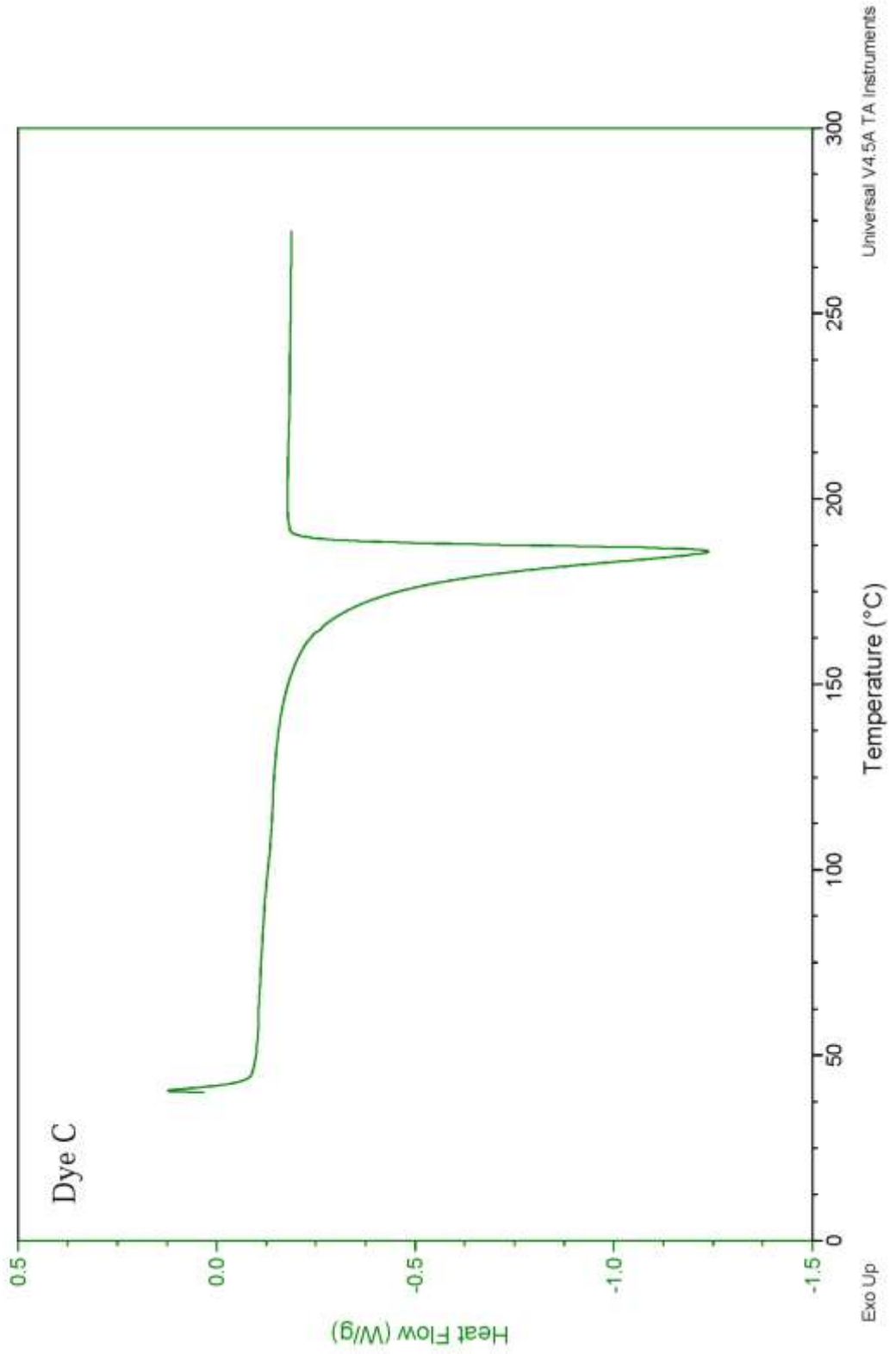
Universal V4.5A TA Instruments



Sample: AW-I-23\_275C  
Size: 3.5000 mg  
Method: Ramp

### DSC

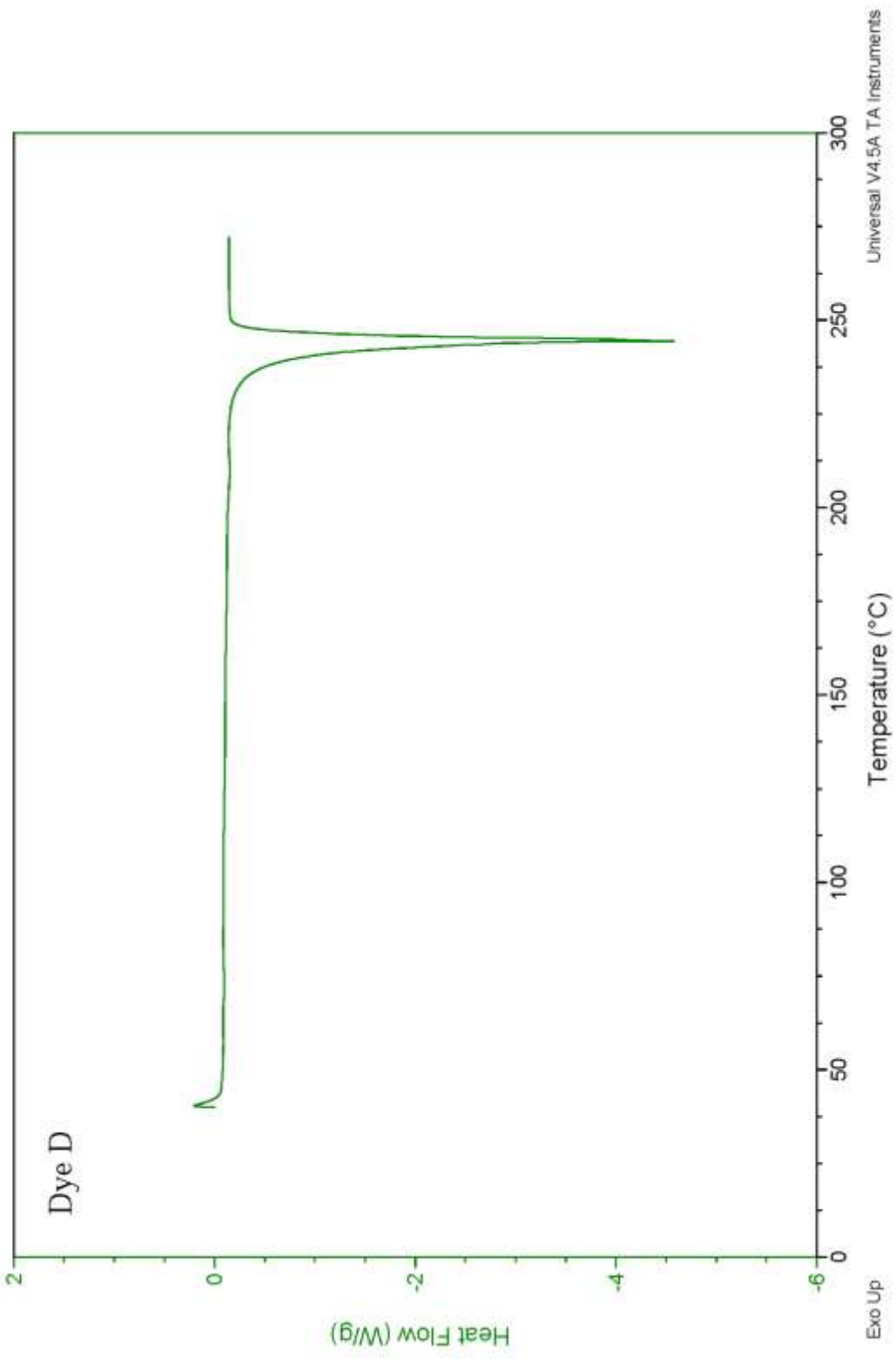
File: C:\...\DSC\AW-I-23\_275C.001  
Operator: BJD  
Run Date: 16-Apr-2016 12:14  
Instrument: DSC Q100 V9.9 Build 303



File: C:\...p-methyl-b-c OPV DSC\_275\_ramp.001  
Operator: AW  
Run Date: 10-Apr-2016 19:50  
Instrument: DSC Q100 V9.9 Build 303

### DSC

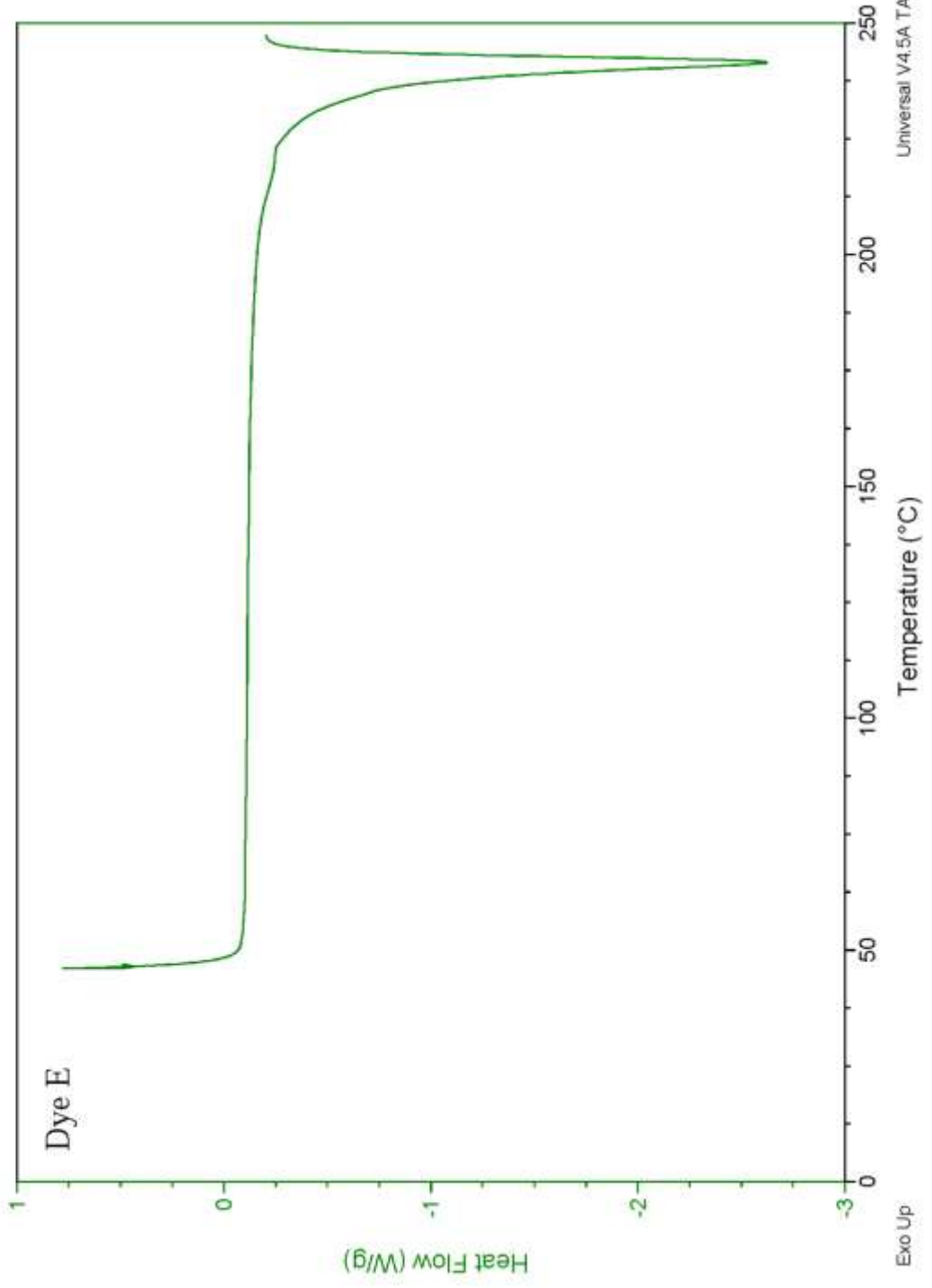
Sample: p-methyl-b-c OPV  
Size: 3.7000 mg  
Method: Ramp  
Comment: ref. pan 0.0527 g



Sample: AW-I-48\_250C  
Size: 3.4000 mg  
Method: Ramp

### DSC

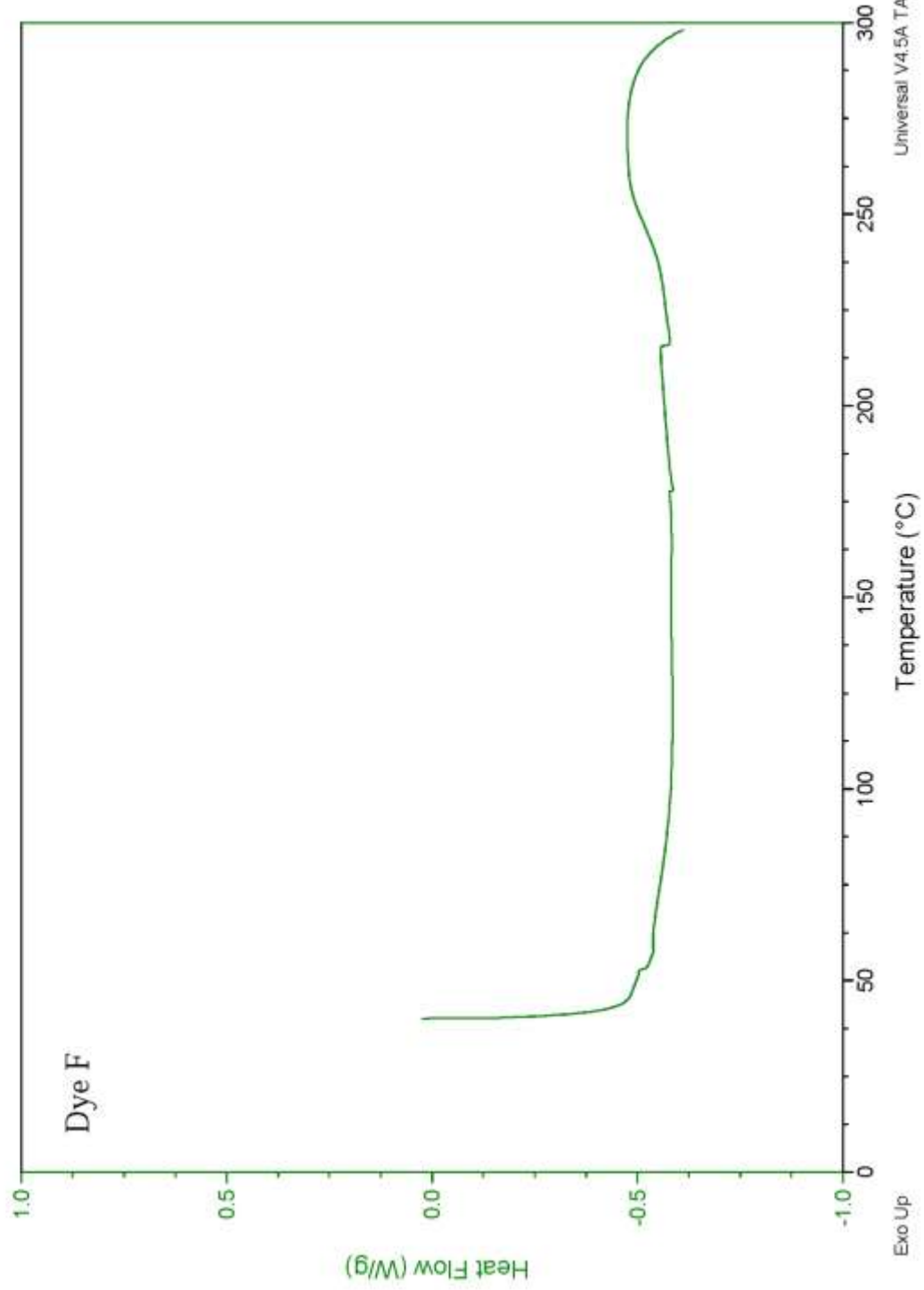
File: C:\... \Digital Notebook\DSC\AW-I-48.003  
Operator: BJD  
Run Date: 16-Apr-2016 11:35  
Instrument: DSC Q100 V9.9 Build 303



Sample: 4-cyano-b-c OPV  
Size: 2.0000 mg  
Method: Heat/Cool/Heat  
Comment: trial 2, no preheat, heat cool heat

### DSC

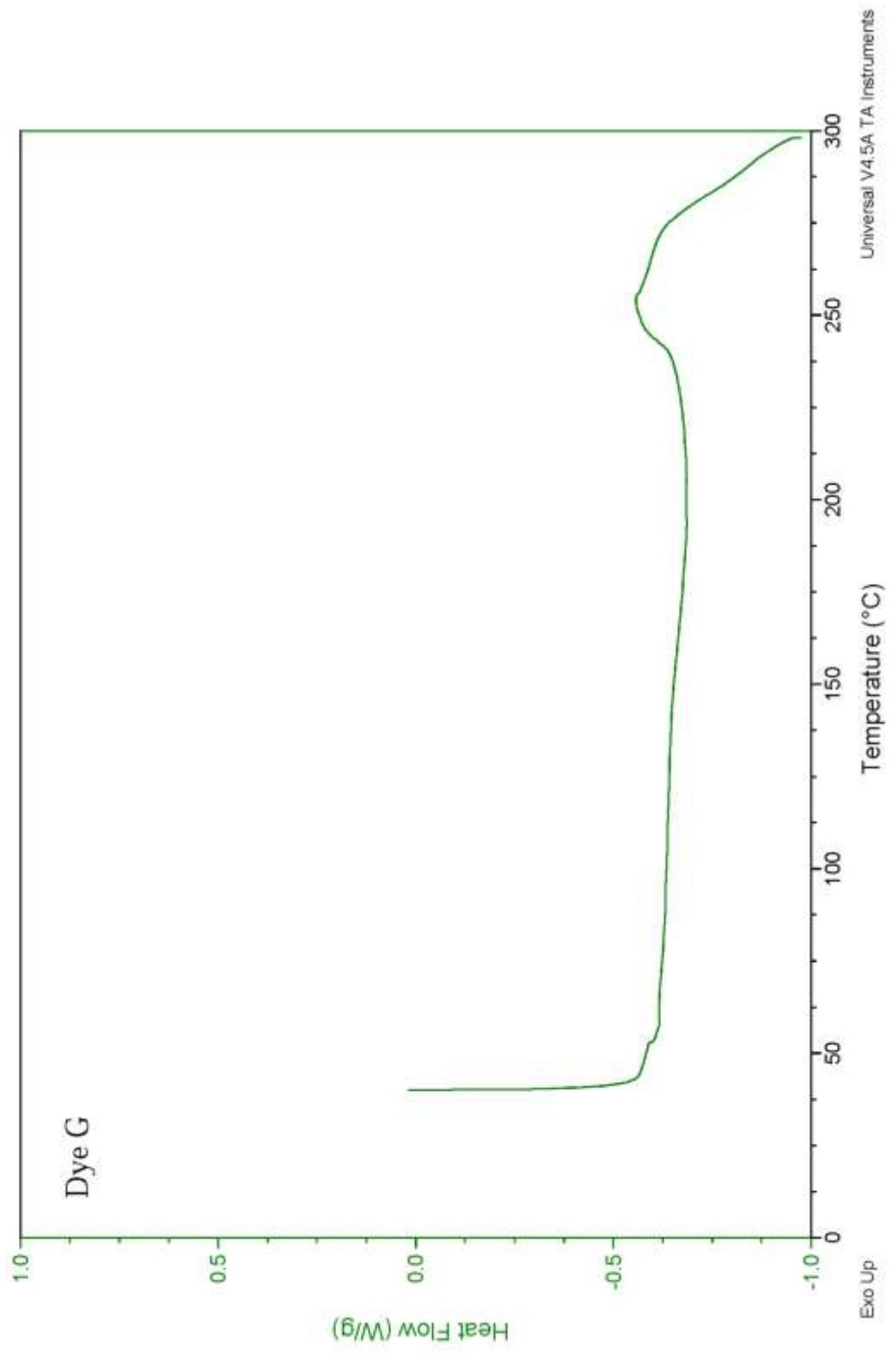
File: 4-cyano-b-c OPV DSC\_300\_heatcoolheat...  
Operator: AW  
Run Date: 28-Apr-2016 15:36  
Instrument: DSC Q100 V9.9 Build 303



Sample: 4-fluoro-b-c OPV  
Size: 2.4000 mg  
Method: Heat/Cool/Heat  
Comment: trial 2, no preheat, heat cool heat

### DSC

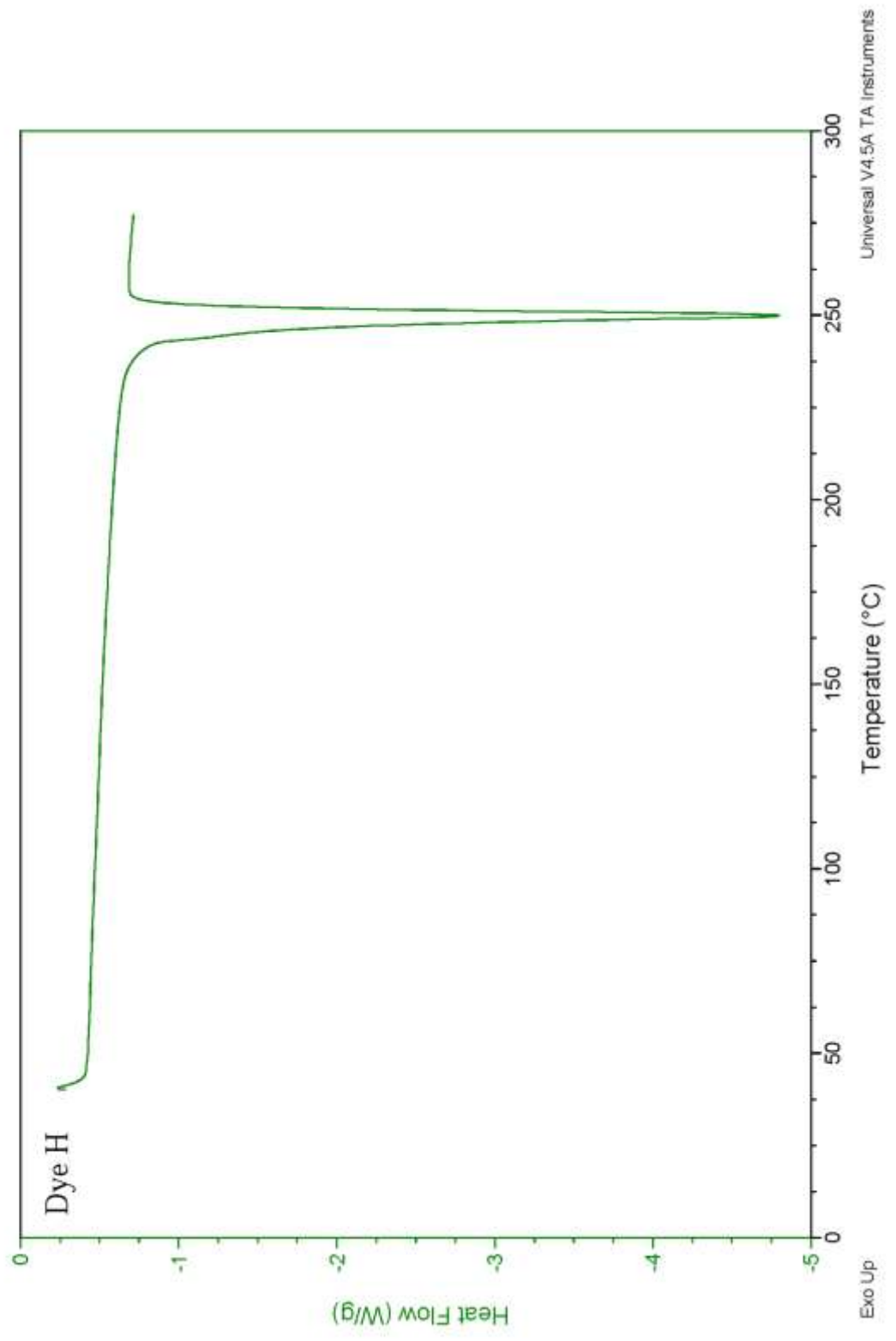
File: 4-fluoro-b-c OPV DSC\_300\_heatcoolhea...  
Operator: AW  
Run Date: 28-Apr-2016 14:41  
Instrument: DSC Q100 V9.9 Build 303



Sample: BJD-III-41\_methoxy  
Size: 3.5000 mg  
Method: Ramp  
Comment: ref. 0.0527 g Ramp after a failed ramp cool ramp cycle

### DSC

File: C:\...AJWB\JD-III-41\_methoxyDSC280.001  
Operator: BJD  
Run Date: 22-Mar-2016 11:08  
Instrument: DSC Q100 V9.9 Build 303



Universal V4.5A TA Instruments